

UNIVERSIDADE ESTADUAL DE MARINGÁ
CENTRO DE CIÊNCIAS DA SAÚDE
DEPARTAMENTO DE ANÁLISES CLÍNICAS E BIOMEDICINA
PROGRAMA DE PÓS-GRADUAÇÃO EM BIOCÊNCIAS E
FISIOPATOLOGIA

GLAUCIA SAYURI ARITA

Virulence and proteomic approaches of *Candida albicans* recovered from
experimental serial systemic candidiasis

Maringá

2018

GLAUCIA SAYURI ARITA

Virulence and proteomic approaches of *Candida albicans* recovered from
experimental serial systemic candidiasis

Dissertação apresentada ao Programa de Pós-Graduação em Biociências e Fisiopatologia do Departamento de Análises Clínicas e Biomedicina, Centro de Ciências da Saúde da Universidade Estadual de Maringá, como requisito parcial para obtenção do título de Mestre em Biociências e Fisiopatologia.

Área de concentração: Biociências e Fisiopatologia Aplicadas à Farmácia

Orientador: Prof.^a Dr.^a Terezinha Inez Estivalet Svidzinski
Co-Orientador: Prof.^a Dr.^a Patrícia de Souza Bonfim de Mendonça

Maringá

2018

Dados Internacionais de Catalogação-na-Publicação (CIP)
(Biblioteca Central - UEM, Maringá – PR., Brasil)

Arita, Glaucia Sayuri

A714v Virulence and proteomic approaches of *Candida albicans* recovered from experimental serial systemic candidiasis/ Glaucia Sayuri Arita.-- Maringá, 2018.

90 f.: il. color. , figs. , tabs.

Orientadora: Prof.a. Dr.a. Terezinha Inez Estivalet Svidzinski.

Coorientadora: Prof.a. Dr.a. Patrícia de Souza Bonfim de Mendonça.

Dissertação (mestrado) - Universidade Estadual de Maringá, Centro de Ciências da Saúde, Programa de Pós-Graduação em Biociências e Fisiopatologia, 2018.

1. Candidíase sistêmica. 2. Passagem seriada. 3. Interação hospedeiro-patógeno. 4. Fatores de virulência. 5. Proteômica. I. Svidzinski, Terezinha Inez Estivalet, orient. II. Mendonça, Patrícia de Souza Bonfim. III. Universidade Estadual de Maringá. Centro de Ciências da Saúde. Programa de Pós-Graduação em Biociências e Fisiopatologia. IV. Título.

CDD 22. ED.616.969

Jane Lessa Monção CRB 1173/97

FOLHA DE APROVAÇÃO

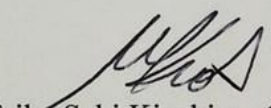
GLAUCIA SAYURI ARITA

Virulence and proteomic approaches of *Candida albicans* recovered from experimental serial systemic candidiasis

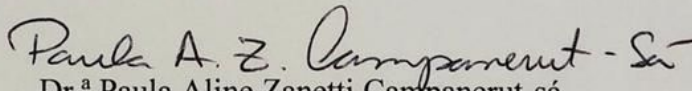
Dissertação apresentada ao Programa de Pós-Graduação em Biociências e Fisiopatologia do Departamento de Análises Clínicas e Biomedicina, Centro de Ciências da Saúde da Universidade Estadual de Maringá, como requisito parcial para obtenção do título de Mestre em Biociências e Fisiopatologia pela Comissão Julgadora composta pelos membros:

COMISSÃO JULGADORA

Dr.^a Terezinha Inez Estivalet Svidzinski
Universidade Estadual de Maringá (Presidente)
Presença remota



Dr.^a Érika Seki Kioshima Cotica
Universidade Estadual de Maringá



Dr.^a Paula Aline Zanetti Campanerut-sá
Universidade Estadual de Maringá

Aprovada em: 18 de dezembro de 2018

Local de Defesa: sala 112-B – Bloco T-20, *campus* da Universidade Estadual de Maringá

DEDICATÓRIA

Dedico este trabalho a todos aqueles que contribuíram para sua realização.

AGRADECIMENTOS

Agradeço primeiramente a Deus por sempre me guiar e me abençoar em todos os momentos.

Aos meus pais, Reinaldo e Alice, as minhas irmãs, Suemi e Kika, pelo apoio, paciência e incentivo nos estudos, por sempre me levar ao laboratório, seja manhã, tarde ou noite e fins de semana. Também, por sempre levar marmita e fruta descascada.

A todos os meus familiares, ditians, batians, tias, tios, primas e primos pelo apoio e compreensão.

A sete pessoas, Namjoon, Jin, Yoongi, Hoseok, Jimin, Taehyung e Jungkook, que me dão muitos momentos de alegria e de “healing”.

Aos meus amigos da graduação, em especial Luciana, Marina, Vanessa e Thaís, pela amizade, mesmo que não conseguimos sempre nos encontrar.

A todos os meus colegas do laboratório de Micologia Médica, em especial, à Karina, Daniella, Franciele, Isis, Pollyanna, Valéria, Raquel, Camila, Lenisa, Janine e Francieli, que foram essenciais para a vivência e para que esse trabalho fosse realizado.

As professoras Paula Campanerut e Luciana Ghiraldi, ao professor Eduardo e ao Jan, por toda ajuda, principalmente na parte de proteômica.

A professora Érika Kioshima que me orientou e me auxiliou desde a graduação e que está sempre disposta a ajudar e a sanar as dúvidas.

A minha co-orientadora professora Patrícia Bonfim-Mendonça que foi a primeira pessoa que eu perguntei se poderia começar a fazer estágio no mico e que foi essencial para a realização desse trabalho. Muito obrigada por sempre poder contar com você.

A minha orientadora professora Terezinha Svidzinski por toda a ajuda que venho recebendo desde 2012 quando entrei no laboratório e também por todas as sugestões que foram enriquecedoras para a realização desse trabalho.

E a todos que contribuíram diretamente ou indiretamente para a realização deste trabalho e para o começo da formação da minha carreira profissional.

EPÍGRAFE

Por vezes sentimos que aquilo que fazemos não é
senão uma gota de água no mar. Mas o mar seria
menor se lhe faltasse uma gota.

(Madre Teresa de Calcuta)

Abordagens de virulência e proteômica de *Candida albicans* recuperadas de candidíase sistêmica seriada experimental

RESUMO

Candida albicans é o principal patógeno isolado de infecções nosocomiais da corrente sanguínea, levando a altas taxas de mortalidade. Além disso, essa espécie expressa alguns fatores de virulência que contribuem para o desenvolvimento de doenças. Estudos anteriores demonstraram ideias sobre a adaptação patógeno-hospedeiro usando um modelo de candidíase sistêmica seriada. Portanto, nós objetivamos inicialmente entender como o processo de infecção seriada poderia influenciar os perfis proteômicos e de virulência em *C. albicans*. Assim, nós infectamos intravenosamente camundongos com células de *C. albicans* e as leveduras recuperadas do rim foram denominadas como P1 (passagem 1). Então, essas células foram usadas para inocular outros camundongos, realizando esse processo até a obtenção de colônias da quinta passagem (P5). Nós observamos um aumento da virulência ao longo das passagens devido à redução significativa no tempo de sobrevivência a partir da passagem 3 (P3). A seguir, nós selecionamos leveduras recuperadas de três passagens (P1, P3 e P4) e da cepa selvagem (WT) para realizar análise proteômica. Um total de 479 proteínas foram obtidas, sendo 56 proteínas diferencialmente abundante em P1, 29 proteínas em maior abundância em P3 e 97 proteínas com maior abundância em P4. Essas proteínas foram categorizadas em relação aos seus potenciais papéis na virulência tais como produção de biofilme, transição levedura-hifa, *switching* fenotípico, proteínas relacionadas à resposta ao estresse e proteínas não caracterizadas. Desse modo, nosso segundo objetivo foi avaliar fenotipicamente fatores de virulência expressos por *C. albicans* recuperada de passagens seriada e comparar com nossos achados proteômicos para entender se essas proteínas encontradas poderiam ser referenciadas como marcadores de virulência. Assim, nós observamos um aumento da carga fúngica recuperada de tecidos infectados com evidente presença de blastoconídios, hifas e áreas inflamatórias no rim ao longo das passagens. Também houve liberação de citocinas pró-inflamatórias fator de necrose tumoral (TNF) e interleucina 6 (IL-6) na resposta imune sistêmica e local, demonstrando uma resposta aguda durante o processo infeccioso. Nós observamos uma estrutura semelhante ao clamidósporo no tecido renal quando estávamos analisando o histopatológico. Então, nós realizamos uma quantificação da produção de clamidósporos *in vitro* que revelou uma tendência crescente na formação dessa estrutura, destacando P3, que foi a passagem com redução significativa do tempo de sobrevivência nos

camundongos. Além disso, cepas recuperadas apresentaram aumentada capacidade para filamentação e produção de biofilme durante as passagens, correlacionando com os dados proteômicos. Além do mais, uma modulação na produção de fosfolipase e proteinase foram observados. Tomados em conjunto, os dados proteômicos encontrados no estudo de *C. albicans* recuperadas após repetidas infecções estão alinhados com os fatores de virulência expressos pelos respectivos isolados. Portanto, essas proteínas deveriam ser investigadas mais aprofundadamente como potenciais marcadores de virulência e consequentemente serem alvos valiosos para o desenvolvimento de novos agentes antifúngicos.

Palavras-chave: Candidíase sistêmica. Passagem seriada. Interação hospedeiro-patógeno. Fatores de virulência. Proteômica.

Virulence and proteomic approaches of *Candida albicans* recovered from experimental serial systemic candidiasis

ABSTRACT

Candida albicans is the main pathogen isolated from nosocomial bloodstream infections, leading to high mortality rates. In addition, this species expresses some virulence factors that contribute to the development of the diseases. Previous studies demonstrated insights into host-pathogen adaptations using a model of serial systemic candidiasis. Therefore, we aimed initially to understand how the process of serial infection could influence proteomic and virulence profiles in *C. albicans*. Thus, we infected intravenously mice with *C. albicans* cells and yeasts recovered from kidney were labelled as P1 (passage 1). Then, these cells were used to inoculate other mice, performing this process until obtaining colonies from the fifth passage (P5). We observed an increase virulence along passages due to significant reduction in survival time from passage 3 (P3) onwards. Next, we selected yeasts recovered from three passages (P1, P3 and P4) and wild-type strain (WT) to perform proteomic analysis. A total of 479 proteins were obtained, being 56 proteins differentially abundant in P1, 29 proteins in greater abundance in P3 and 97 proteins with higher abundance in P4. These proteins were categorized in relation to their potential roles in the virulence such as biofilm production, yeast-to-hyphae transition, phenotypic switching, proteins related to stress response and uncharacterized proteins. In this way, our second goal was to phenotypically evaluate virulence factors expressed by *C. albicans* recovered from serial passages and to compare with our proteomic findings, to understand if these proteins found could be referenced as virulence markers. Thus, we observed an increased fungal burden recovered from infected tissues with evident presence of blastoconidia, hyphae and inflammatory areas in the kidney along the passages. There was also release of proinflammatory cytokines Tumor Necrosis Factor (TNF) and Interleukin 6 (IL-6) in system and local immune response, demonstrating an acute response during the infectious process. We observed a chlamydospore-like structure in the renal tissue when we were analyzing the histopathological. Then, we performed a quantification of chlamydospores production *in vitro* that revealed an increasing trend in formation of this structure, highlighting P3, which was the passage with significant survival time reduction in mice. Moreover, recovered strains presented increased capacity of filamentation and biofilm production during passages correlating with proteomics data. Furthermore, a modulation of phospholipase and proteinase production was observed. Taken together, proteomics data found in this study of *C. albicans* recovered after repeated infections are aligned with the virulence factors expressed by the respective isolates.

Therefore, these proteins should be further investigate as potential virulence markers and consequently be valuable targets for the development of new antifungal agents.

Keywords: Systemic candidiasis. Serial passage. Host-pathogen interaction. Virulence factors. Proteomics.

Capítulos da dissertação elaborados e formatados conforme as normas da ABNT NBR 14724: 2011 e artigos conforme as normas das revistas científicas.

Disponível em:

- Manuscript 1 (Breaking report): *Celullar Microbiology*

<https://onlinelibrary.wiley.com/page/journal/14625822/homepage/forauthors.html>

- Manuscript 2: *Future Microbiology*

<https://www.futuremedicine.com/authorguide>

TABLE OF CONTENTS

CHAPTER I.....	12
1. INTRODUCTION.....	12
1.1 Candidemia	12
1.2 <i>Candida</i> spp.	13
1.3 <i>C. albicans</i> virulence factors	13
1.4 Proteomics	16
2. JUSTIFICATION	18
3. OBJECTIVES.....	19
3.1 General objective	19
3.2 Specific objectives	19
REFERENCES	20
CHAPTER II	28
Manuscript 1 (Breaking report): Serial systemic <i>Candida albicans</i> infection highlighted by proteomics	28
Manuscript 2: Insights into <i>Candida albicans</i> virulence factors after serial systemic candidiasis	66
CHAPTER III.....	89
4. CONCLUSIONS	89
5. FUTURE PERSPECTIVES	90

CHAPTER I

1. INTRODUCTION

1.1 Candidemia

According to the Global Action Fund for Fungal Infections⁽¹⁾, over 300 million people are affected by a serious fungal infection worldwide. Among them, cryptococcal meningitis, pneumocystis pneumonia, disseminated histoplasmosis, invasive aspergillosis, invasive candidiasis, chronic pulmonary aspergillosis and severe asthma with fungal sensitization (SAFS) lead to an estimate of 1,600,000 million of deaths. Invasive candidiasis affects more than 750,000 people with approximately 40% of deaths when treated, accounting for more than 350,000 deaths.

Invasive candidiasis can be manifested by candidemia, deep tissue infection (intra-abdominal abscess, peritonitis, osteomyelitis), or disseminated disease with deep organ involvement⁽²⁾. A multicenter prospective study conducted in seven Latin American countries (Brazil, Chile, Argentina, Ecuador, Colombia, Venezuela, Honduras) revealed high incidence of candidemia, with an overall incidence of 1.18 cases per 1,000 admissions and 0.23 cases per 1,000 patients-day⁽³⁾. Similarly, Brazil showed an incidence of 1.38 cases per 1,000 admissions and 0.26 cases per 1,000 patients-day⁽³⁾. Furthermore, *Candida* spp. were the seventh most prevalent pathogen among nosocomial bloodstream infection (nBSI) in Brazil leading to a mortality rate of 72%⁽⁴⁾. In the United States, *Candida* species were the fourth most isolated agents in nBSI with an incidence of 4.6 per 10,000 hospital admissions and with mortality rate of 39.2%⁽⁵⁾.

Several underlying conditions are associated with candidemia such as cancer, gastrointestinal, neurologic and pulmonary diseases⁽³⁻⁷⁾. Furthermore, predisposing factors such as use of antimicrobial agents, corticosteroid, chemotherapy, age, previous colonization, gastric acid suppression, central venous catheter (CVC), urinary catheter, total parenteral nutrition (TPN), neutropenia, gastrointestinal surgery, mechanical ventilation, renal failure (hemodialysis), malnutrition, hospital or intensive care unit (ICU) stay and severity of disease increase the risk for acquiring candidemia^(3, 4, 6, 7). It is worth noting that hospitalization in the ICU facilitate dissemination of *Candida* among patients⁽⁷⁾. Risk of cross-transmission between healthcare workers (HCWs) and hospitalized patients, and also, between HCWs and ICU

surfaces have been previously described⁽⁸⁻¹⁰⁾. Abdeljelil et al. (2012)⁽⁹⁾ correlated invasive candidiasis in neonates and HCWs as the source of infection. They also revealed occurrence of genetic changes in DNA fragments denominated microevolution in a catheter-related candidemia, as one blood isolate and the first catheter isolate from the same patient exhibited minor band differences. Moreover, Sakita et al. (2017)⁽¹⁰⁾ demonstrated enhanced virulence traits among strains isolated from HCWs' hands and ICU surfaces and these isolates had strong intra-species similarities, highlighting the importance of cross-transmission of *Candida spp.* in hospital environments.

1.2 *Candida spp.*

Candida is a genus belonging to phylum Ascomycota, subphylum Saccharomycotina, class Saccharomycetes, order Saccharomycetales and family Saccharomycetaceae⁽¹¹⁾. There are more than 200 known species and over 40 can cause disease⁽¹²⁾. Among them, *C. albicans* remains as the main pathogen of nosocomial candidemia, although species non-*C. albicans* such as *C. parapsilosis*, *C. tropicalis*, *C. glabrata* and *C. krusei* are increasing^(3-5, 13).

C. albicans is a polymorphic fungus found in unicellular yeast form, pseudohyphal and true hyphal^(14, 15). It also can produce a large, spherical and thick-walled structure called chlamydospore which has been used for identification of *Candida* species^(3, 8, 16).

It is well known *C. albicans* inhabits human microbiota of the gastrointestinal tract, vaginal mucosa, oral cavity and skin⁽¹⁷⁻²¹⁾. However, an imbalance of the immune system and/or perturbations of mucosal microbiota, make *Candida* transit from commensal to opportunistic form, contributing to the appearance of disease that ranges from superficial to potentially fatal disseminated candidiasis^(2, 14, 15). In addition, this species expresses several virulence factors such as adherence, morphogenesis (yeast-to-hyphae transition), secretion of hydrolytic enzymes, biofilm formation, phenotypic switching, and fitness attributes such as adaptations to environmental changes in pH, nutrients, stress, important for the establishment of the disease^(2, 14, 15).

1.3 *C. albicans* virulence factors

First step to *C. albicans* cause infection is related to its ability to adherence host tissue by proteins denominated adhesins. Among them, agglutinin-like sequence family (Als) is composed by eight proteins (Als1 to Als7 and Als9), with emphasis in Als3 that has been

reported to be present in germ tube and its blockade by antibodies led to *C. albicans* not to adhere to epithelial and endothelial cells^(22, 23). In addition, Hwp1 (hyphal wall protein 1) is an important adhesin expressed in germ tubes and hyphae, and mutant strain *hwp1/hwp1* exhibited reduced adherence in cells and showed attenuated virulence in a mouse model of systemic candidiasis^(15, 24, 25). Moreover, Als3 and Hwp1 have demonstrated a role during biofilm formation *in vivo* and *in vitro*^(15, 26-28).

During invasion to the tissue, *C. albicans* changes its morphology from yeast to hyphae form, which has been a crucial step for infection as strain unable to filament were avirulent in animals model of systemic candidiasis^(29, 30). This transition is induced by several conditions that mimic host environment such as serum, temperature of 37°C, neutral pH and 5% CO₂^(31, 32). Other laboratory conditions such as Lee's medium, Spider medium and tissue culture make yeast cells undergo switch to hyphae form as well⁽³²⁾. Furthermore, filamentation is required for escape killing by macrophages since a nonfilamentous mutant strain was unable to escape from macrophages after phagocytosis⁽³³⁾.

In addition to filamentation, secretion of hydrolytic enzymes such as phospholipase B and secreted aspartyl proteinases (Sap) by *C. albicans* are important for pathogenesis⁽³⁴⁾. Saps are encoded by 10 genes (*SAP1-SAP10*) and their roles are attributed in nutrients acquisition for the cells, in invasion tissue and in escape from immune system^(34, 35). Saps are capable of digesting host tissue and human endothelial extracellular matrix that contribute to *Candida* cells cross the bloodstream and to disseminate into deep organs⁽³⁶⁾. Moreover, they can cleavage immunoglobulins and complement C3 molecules which are important proteins in humoral immune response^(37, 38). Saps 1 to 3 have optimal activity in lower pH (2.5–5.5) and Saps 4 to 6 in higher pH (3.0–7.0) enabling fungus to adapt in different tissues⁽³⁴⁾. There are some divergences about proteinase impact on virulence. Hube et al. (1997)⁽³⁹⁾ demonstrated that null mutants in *SAP1*, *SAP2* and *SAP3* were less virulent in models of systemic candidiasis. Furthermore, the triple deletion of *SAP4*, *SAP5* and *SAP6* genes attenuated *C. albicans* virulence⁽⁴⁰⁾, and expression of these genes were associated predominantly with hyphal cells⁽³⁵⁾. In contrast, Correia et al. (2010)⁽⁴¹⁾ did not find significant differences in survival time among mice infected by wild-type and $\Delta sap123$ mutant or $\Delta sap456$ strains, thus, Sap1 to Sap6 did not play a major role in virulence during disseminated candidiasis. These authors related this difference due to the technique used for mutant construction, while Hube et al. (1997)⁽³⁹⁾ used Ura-blaster *sap* mutants, in which the ectopic insertion of *URA3* could have influenced the

attenuated virulence, Correia et al. (2010)⁽⁴¹⁾ used SAT1-flipping strategy that is not related to *URA3* gene. Whether or not proteinases increase *C. albicans* virulence, several studies have shown proteinase and phospholipase activities in strains recovered from patients with candidemia⁽⁴²⁻⁴⁵⁾.

Phospholipase family is composed by four classes (A, B, C and D), but only class B which contains five members (PLB1-5) seems to be extracellular and could contribute for pathogenicity^(46, 47). This enzyme is capable of degrading phospholipids from cell membranes and lysophospholipids releasing free fatty acids^(46, 48). Theiss et al. (2006)⁽⁴⁸⁾ demonstrated upregulation of *PLB5* gene during filamentation assay in Lee's media in germ tubes grown at 37°C, pH 6.8. Furthermore, *caplb5* null mutant strain showed attenuated virulence in a murine model of systemic candidiasis, confirming its relation with virulence⁽⁴⁸⁾. Leidich et al. (1998)⁽⁴⁹⁾ demonstrated expression of *PLB* *in vivo* using an antiserum that bound to PLB in the kidney tissue infected with *C. albicans*. Moreover, deletion of *caPLB1* attenuated virulence in murine model of disseminated candidiasis, displaying longer survival time and lower fungal burden when compared to mice infected with parental strain⁽⁴⁹⁾. Mutant strains were also cleared faster from the kidneys. In addition, they also compared ability to penetrate endothelial and epithelial cells, although both mutant strain and wild-type produced germ tubes and adhered to the cells, the strain lacking PLB had lower penetration than wild-type SC5314⁽⁴⁹⁾. These findings demonstrate a role of phospholipase as a virulence factor possibly due to its capacity of invade and damage tissue^(49, 50).

Biofilm formation by *C. albicans* involves four steps: first, adhesion of yeasts cells on abiotic or biotic surface; second, proliferation of these cells and formation of pseudohyphae and hyphae; third, accumulation of extracellular matrix during maturation; and fourth, dispersion of non-adherent yeast cells^(15, 51). Furthermore, dispersed cells from biofilm, which are responsible for candidemia and dissemination, showed higher adherence, filamentation and ability to form biofilm, and also, were more virulent in a murine model of hematogenously disseminated candidiasis than their planktonic counterparts⁽⁵²⁾. Knowing that *C. albicans* has ability to form biofilm in a variety surfaces, highlighting, implanted medical devices (central venous catheter, joint prostheses, cardiovascular devices, central nervous systems devices, urinary catheters, dentures, contact lenses), studies suggest these devices as potential source of infection. Removal of these devices are necessities to cure infection; however, it is not always possible, leading to complications^(9, 53-55). Furthermore, CVC-related infection probably due to

biofilm formation is related to persistent candidemia⁽⁵⁶⁻⁵⁸⁾ and antifungal resistance⁽⁵⁹⁻⁶¹⁾. Hawser and Douglas (1995)⁽⁵⁹⁾ found biofilm of *C. albicans* exhibited high resistance to antifungal agents such as amphotericin B, fluconazole, flucytosine, itraconazole and ketoconazole. These findings denote the importance of studying continuously virulence factors expressed by *C. albicans*.

1.4 Proteomics

The classical proteomic technique is based on two-dimensional gel electrophoresis (2-DE) but it is laborious and time-consuming. The proteins are separated according to their isoelectric point (pI) in the first dimension and molecular weight (MW) in the second dimension⁽⁶⁵⁻⁶⁷⁾. With the advancement of mass spectrometry, non-based gel techniques are used for sensitive and accurate quantification. MS is a high-throughput method that identify proteins based on their mass to charge ratio (m/z) spectra⁽⁶⁵⁻⁶⁷⁾. Among MS techniques, there are matrix-assisted laser desorption ionization-time-of-flight (MALDI-TOF), electrospray ionization tandem mass spectrometry (ESI-MS/MS), liquid chromatography tandem mass spectrometry (LC-MS/MS), surface enhanced laser desorption ionization (SELDI), isotope coded affinity tags (ICAT), stable isotope labeling with amino acids in cell culture (SILAC) and isobaric tag for relative, absolute quantification (iTRAQ) and tandem mass tag (TMT)⁽⁶⁶⁻⁶⁸⁾. The last four are label-based quantitative proteomics. Another approach for quantification is the label-free quantitative proteomics that gives an estimated abundance of proteins and is provided by several software such as Proteome Discoverer, Scaffold, Progenesis and MaxQuant^(69, 70). This last one is freely available and exhibits accurate and precise quantification based on peptide ion signal peak intensity⁽⁷⁰⁾. Thus, label-free proteomics can be applied in diverse studies aiming discovery of biomarkers and targets for antimicrobial agents.

The omics transcriptomics and proteomics have been a useful tool to study host-pathogen interactions⁽⁶²⁾. There are many studies regarding genes expressed during experiments with *C. albicans*. For instance, García-Sánchez et al. (2004)⁽⁶³⁾ studied transcript profiles of *C. albicans* biofilms from different conditions of flow (continuous or limited), oxygenation (microfermentor, microtiter plate, catheter disks, flask), and glucose concentration (0.4% and 2.0%) and compared with planktonic transcriptome. They found 325 genes differentially expressed between biofilm and planktonic conditions, with 214 genes being overexpressed and 111 genes underexpressed in biofilm. Among them, they observed overexpressed genes relating

to protein synthesis, sulfur amino acids (amino acid metabolism), carbohydrate metabolism and energy. On the other hand, genes related to cell cycle, DNA processing and glucose repression were underexpressed. Thus, they found genes related to pathogenesis that contribute to the understanding of virulence in *C. albicans*.

Genomics provide valuable knowledge at gene level; however, for a deeper insight about which effector or molecule are in charge to determined condition, proteomics is necessary⁽⁶²⁾. Thus, proteome analysis is an important approach for comprehensive characterization of dynamic variations that occur during adaptation of microorganisms under different conditions. Aoki et al. (2013)⁽⁶⁴⁾ performed a quantitative time-course proteomics using liquid chromatography-tandem mass spectrometry (LC-MS/MS) system during filamentation of *C. albicans* in fetal bovine serum (FBS) from 0 to 180 min. After extraction and digestion of proteins, they were labeled with different TMT (tandem mass tag) for each group (0, 30, 60, 120, 180 and internal control for quantification). They identified and quantified 1024 proteins, in which 22 proteins were upregulated during filamentation when compared to proteins incubated in YPD media, and 28 proteins were uniquely found in the FBS series. Proteins related to energy, oxidative stress response, iron acquisition were induced during incubation with serum. In addition, they characterized an unknown protein named blood-induced peptide (Blp1) that exhibited higher stress-tolerance and might contribute to virulence of *C. albicans*. Therefore, omics provide data that contribute to the elucidation of how pathogen adapts to the host environment during infection.

2. JUSTIFICATION

C. albicans is the main pathogen associated to candidemia, leading to high mortality rates. It is well known that this species expresses some virulence attributes such as adherence, yeast-to-hyphae transition, secretion of phospholipases and proteinases and ability to form biofilm that contribute to pathogenesis. It is believed that the contact between *Candida* cells and host and their ability to adapt to different conditions could modulate expression of these factors and could result in a more pathogenic microorganism. There are few studies involving the serial model of systemic infection caused by *C. albicans* and they provided some insights into host-pathogen adaptations. Furthermore, with the advancement proteomic studies, mechanisms of the interaction between host and pathogen have been described. To the best of our knowledge, this is the first study to assess proteomic profile of the *C. albicans* after serial passage in a systemic candidiasis model. Therefore, in view of the increase and severity of invasive infections caused by *C. albicans*, this study focus on elucidate the proteomic and phenotypic changes in *C. albicans* recovered from serial systemic candidiasis.

3. OBJECTIVES

3.1 General objective

To evaluate proteomic and phenotypic changes caused by host-pathogen interaction after a model of serial systemic *C. albicans* infection.

3.2 Specific objectives

- To perform intravenous challenge of *C. albicans* in a murine model of serial infection;
- To evaluate pathogenicity of *C. albicans* through survival curve experiment;
- To analyze proteomic profiles of *C. albicans* recovered from infection;
- To assess fungal burden and histopathological alterations;
- To evaluate immune response by cytokines quantification;
- To analyze *in vitro* virulence profile such as chlamydospore production, filamentation, activity of hydrolytic enzymes, and biofilm formation.

REFERENCES

1. GLOBAL ACTION FUNDI FOR FUNGAL INFECTIONS. Fungal disease frequency. **Gaffi**, 2018. Retrieved from:<<https://www.gaffi.org/why/fungal-disease-frequency/>>. Accessed in: 20 nov. 2018.
2. PAPPAS, P. G. et al. Invasive candidiasis. **Nature Reviews Disease Primers**, v. 4, p. 18026, 2018. DOI: <http://dx.doi.org/10.1038/nrdp.2018.26>.
3. NUCCI, M. et al. Epidemiology of candidemia in Latin America: a laboratory-based survey. **PLoS ONE**, v. 8, n. 3, e59373, 2013. DOI: <https://doi.org/10.1371/journal.pone.0059373>.
4. DOI, A. M. et al. Epidemiology and microbiologic characterization of nosocomial candidemia from a brazilian national surveillance program. **PLoS ONE**, v. 11, n. 1, e0146909, 2016. DOI: <https://doi.org/10.1371/journal.pone.0146909>.
5. WISPLINGHOFF, H. et al. Nosocomial bloodstream infections in US hospitals: analysis of 24,179 cases from a prospective nationwide surveillance study. **Clinical Infectious Diseases**, v. 39, n. 3, p. 309-317, 2004. DOI: <https://doi.org/10.1086/421946>. Erratum in: **Clinical Infectious Diseases**, v. 39, n. 7, p. 1093, 2004. DOI: <https://doi.org/10.1086/425328>. Erratum in: **Clinical Infectious Diseases**, v. 40, n. 7, p. 1077, 2005. DOI: <https://doi.org/10.1086/429630>.
6. WISPLINGHOFF, H. et al. Nosocomial bloodstream infections due to *Candida* spp. in the USA: species distribution, clinical features and antifungal susceptibilities. **International Journal of Antimicrobial Agents**, v. 43, n. 1, p. 78-81, 2014. DOI: <https://doi.org/10.1016/j.ijantimicag.2013.09.005>.
7. PFALLER, M. A.; DIEKEMA, D. J. Epidemiology of invasive candidiasis: a persistent public health problem. **Clinical Microbiology Reviews**, v. 20, n. 1, p. 133-163, 2007. DOI: <https://doi.org/10.1128/CMR.00029-06>.
8. ABDELJELIL, J. B. et al. Molecular typing of *Candida albicans* isolates from patients and health care workers in a neonatal intensive care unit. **Journal of Applied Microbiology**, v. 111, n. 5, p. 1235-1249, 2011. DOI: <https://doi.org/10.1111/j.1365-2672.2011.05121.x>.
9. ABDELJELIL, J. B. et al. Investigation of a cluster of *Candida albicans* invasive candidiasis in a neonatal intensive care unit by pulsed-field gel electrophoresis. **The**

- Scientific World Journal**, v. 2012, p. 1-7, 2012. DOI: <https://doi.org/10.1100/2012/138989>.
10. SAKITA, K. M. et al. Healthcare workers' hands as a vehicle for the transmission of virulent strains of *Candida* spp.: a virulence factor approach. **Microbial Pathogenesis**, v. 113, p. 225-232, 2017. DOI: <https://doi.org/10.1016/j.micpath.2017.10.044>.
 11. DE HOOG, G. S. et al. **Atlas of clinical fungi** (version 4.1.4). Ulltrecht, NL: Centraalbureau voor Schimmelcultures, 2018.
 12. JOHNSON, E. M. Rare and emerging *Candida* species. **Current Fungal Infection Reports**, v. 3, n. 3, p. 152-159, 2009. DOI: <https://doi.org/10.1007/s12281-009-0020-z>.
 13. LAMOTH, F. et al. Changes in the epidemiological landscape of invasive candidiasis. **Journal of Antimicrobial Chemotherapy**, v. 73, n. 1, p. i4-i13, 2018. DOI: <https://doi.org/10.1093/jac/dkx444>.
 14. CALDERONE, R. A.; FONZI, W. A. Virulence factors of *Candida albicans*. **Trends in Microbiology**, v. 9, n. 7, p. 327-335, 2001. DOI: [https://doi.org/10.1016/S0966-842X\(01\)02094-7](https://doi.org/10.1016/S0966-842X(01)02094-7).
 15. MAYER, F. L.; WILSON, D.; HUBE, B. *Candida albicans* pathogenicity mechanisms. **Virulence**, v. 4, n. 2, p. 119-128, 2013. DOI: <https://doi.org/10.4161/viru.22913>.
 16. NAVARATHNA, D. H. M. L. P. et al. *Candida albicans* ISW2 regulates chlamydospore suspensor cell formation and virulence *in vivo* in a mouse model of disseminated candidiasis. **PLoS ONE**, v. 11, n. 10, e0164449, 2016. DOI: <https://doi.org/10.1371/journal.pone.0164449>.
 17. HALL, R. A.; NOVERR, M. C. Fungal interactions with the human host: exploring the spectrum of symbiosis. **Current Opinion in Microbiology**, v. 40, p. 58-64, 2017. DOI: <https://doi.org/10.1016/j.mib.2017.10.020>.
 18. NASH, A. K. et al. The gut mycobiome of the Human Microbiome Project healthy cohort. **Microbiome**, v. 153, n. 5, p. 1-13, 2017. DOI: <https://doi.org/10.1186/s40168-017-0373-4>.

19. BRADFORD, L. L.; RAVEL, J. The vaginal mycobiome: A contemporary perspective on fungi in women's health and diseases. **Virulence**, v. 8, n. 3, p. 342-351, 2017. DOI: <http://dx.doi.org/10.1080/21505594.2016.1237332>.
20. PETERS, B. A. et al. The oral fungal mycobiome: characteristics and relation to periodontitis in a pilot study. **BMC Microbiology**, v. 157, n. 17, p. 1-11, 2017. DOI: <https://doi.org/10.1186/s12866-017-1064-9>.
21. LIMON, J. J.; SKALSKI, J. H.; UNDERHILL, D. M. Commensal fungi in health and disease. **Cell Host & Microbe**, v. 22, n. 2, p. 156-165, 2017. DOI: <https://doi.org/10.1016/j.chom.2017.07.002>.
22. COLEMAN, D. A. et al. Monoclonal antibodies specific for *Candida albicans* Als3 that immunolabel fungal cells in vitro and in vivo and block adhesion to host surfaces. **Journal of Microbiological Methods**, v. 78, n. 1, p. 71-78, 2009. DOI: <https://doi.org/10.1016/j.mimet.2009.05.002>.
23. COTA, E.; HOYER, L. L. The *Candida albicans* agglutinin-like sequence family of adhesins: functional insights gained from structural analysis. **Future Microbiology**, v. 10, n. 10, p. 1635-1648, 2015. DOI: <https://doi.org/10.2217/fmb.15.79>.
24. STAAB, J. F. et al. Adhesive and mammalian transglutaminase substrate properties of *Candida albicans* Hwpl. **Science**, v. 283, n. 5407, p. 1535-1538, 1999. DOI: <https://doi.org/10.1126/science.283.5407.1535>.
25. SUNDSTROM, P.; CUTLER, J. E.; STAAB, J. F. Reevaluation of the role of *HWPI* in systemic candidiasis by use of *Candida albicans* strains with selectable marker *URA3* targeted to the *ENO1* locus. **Infection and Immunity**, v. 70, n. 6, p. 3281-3283, 2002. DOI: <https://doi.org/10.1128/IAI.70.6.3281-3283.2002>.
26. NOBILE, C. J. et al. Critical role of Bcr1-dependent adhesins in *C. albicans* biofilm formation *in vitro* and *in vivo*. **PLoS Pathogens**, v. 2, n. 7, e63, 2006a. DOI: <https://doi.org/10.1371/journal.ppat.0020063>.
27. NOBILE, C. J. et al. Function of *Candida albicans* adhesin Hwp1 in biofilm formation. **Eukaryotic Cell**, v. 5, n. 10, p. 1604–1610, 2006b. DOI: <https://doi.org/10.1128/EC.00194-06>.

28. NOBILE, C. J. et al. Complementary adhesin function in *C. albicans* biofilm formation. **Current Biology**, v. 18, n. 14, p. 1014-1024, 2008. DOI: <https://doi.org/10.1016/j.cub.2008.06.034>.
29. LO, H. J. et al. Nonfilamentous *C. albicans* mutants are avirulent. **Cell**, v. 90, n. 5, p. 939-949, 1997. DOI: [https://doi.org/10.1016/S0092-8674\(00\)80358-X](https://doi.org/10.1016/S0092-8674(00)80358-X).
30. BI, S. et al. *SDH2* is involved in proper hypha formation and virulence in *Candida albicans*. **Future Microbiology**, v. 13, n. 10, p. 1141-1156, 2018. DOI: <https://doi.org/10.2217/fmb-2018-0033>.
31. SUDBERY, P.; GOW, N.; BERMAN, J. The distinct morphogenic states of *Candida albicans*. **Trends in Microbiology**, v. 12, n. 7, p. 317-324, 2004. DOI: <https://doi.org/10.1016/j.tim.2004.05.008>.
32. SUDBERY, P. E. Growth of *Candida albicans* hyphae. **Nature Reviews Microbiology**, v. 9, p. 737-748, 2011. DOI: <https://doi.org/10.1038/nrmicro2636>.
33. LORENZ, M. C.; BENDER, J. A.; FINK, G. R. Transcriptional response of *Candida albicans* upon internalization by macrophages. **Eukaryotic Cell**, v. 3, n. 5, p. 1076-1087, 2004. DOI: <https://doi.org/10.1128/EC.3.5.1076-1087.2004>.
34. NAGLIK, J. R.; CHALLACOMBE, S. J.; HUBE, B. *Candida albicans* secreted aspartyl proteinases in virulence and pathogenesis. **Microbiology and Molecular Biology Reviews**, v. 67, n. 3, p. 400-428, 2003. DOI: <https://doi.org/10.1128/MMBR.67.3.400-428.2003>.
35. FELK, A. et al. *Candida albicans* hyphal formation and the expression of the Efg1-regulated proteinases Sap4 to Sap6 are required for the invasion of parenchymal organs. **Infection and Immunity**, v. 70, n. 7, p. 3689-3700, 2002. DOI: <https://doi.org/10.1128/IAI.70.7.3689-3700.2002>.
36. MORSCHHÄUSER, J. Degradation of human subendothelial extracellular matrix by proteinase-secreting *Candida albicans*. **FEMS Microbiology Letters**, v. 153, n. 2, p. 349-355, 1997. DOI: <https://doi.org/10.1111/j.1574-6968.1997.tb12595.x>.
37. RÜCHEL, R. Cleavage of immunoglobulins by pathogenic yeasts of the genus *Candida*. **Microbiological Sciences**, v. 3, n. 10, p. 316-319, 1986.

38. KAMINISHI, H. et al. Degradation of humoral host defense by *Candida albicans* proteinase. **Infection and Immunity**, v. 63, n. 3, p. 984-988, 1995.
39. HUBE, B. et al. Disruption of each of the secreted aspartyl proteinase genes *SAP1*, *SAP2*, and *SAP3* of *Candida albicans* attenuates virulence. **Infection and Immunity**, v. 65, n. 9, p. 3529-3538, 1997.
40. SANGLARD, D. et al. A triple deletion of the secreted aspartyl proteinase genes *SAP4*, *SAP5*, and *SAP6* of *Candida albicans* causes attenuated virulence. **Infection and Immunity**, v. 65, n. 9, p. 3539-3546, 1997.
41. CORREIA, A. et al. Limited role of secreted aspartyl proteinases Sap1 to Sap6 in *Candida albicans* virulence and host immune response in murine hematogenously disseminated candidiasis. **Infection and Immunity**, v. 78, n. 11, p. 4839-4849, 2010. DOI: <https://doi.org/10.1128/IAI.00248-10>.
42. MANDELBLAT, M. et al. Phenotypic and genotypic characteristics of *Candida albicans* isolates from bloodstream and mucosal infections. **Mycoses**, v. 60, n. 8, p. 534-545, 2017. DOI: <https://doi.org/10.1111/myc.12623>.
43. CANELA, H. M. S. et al. Prevalence, virulence factors and antifungal susceptibility of *Candida* spp. isolated from bloodstream infections in a tertiary care hospital in Brazil. **Mycoses**, v. 61, n. 1, p. 11-21, 2018. DOI: <https://doi.org/10.1111/myc.12695>.
44. TAY, S. T. et al. Proteinase, phospholipase, biofilm forming abilities and antifungal susceptibilities of Malaysian *Candida* isolates from blood cultures. **Medical Mycology**, v. 49, n. 5, p.556-560, 2011. DOI: <https://doi.org/10.3109/13693786.2010.551424>.
45. SARIGUZEL, F. M. Investigation of the relationship between virulence factors and genotype of *Candida* spp. isolated from blood cultures. **Journal of Infection in Developing Countries**, v. 9, n. 8, p. 857-864, 2015. DOI: <https://doi.org/10.3855/jidc.5359>.
46. NIEWERTH, M.; KORTING, H. C. Phospholipases of *Candida albicans*. **Mycoses**, v. 44, n. 9-10, p. 361-367, 2002. DOI: <https://doi.org/10.1046/j.1439-0507.2001.00685.x>.
47. MAVOR, A. L.; THEWES, S.; HUBE, B. Systemic fungal infections caused by *Candida* species: epidemiology, infection process and virulence attributes. **Current Drug Targets**, v. 6, n. 8, p. 863-874, 2005. DOI: <https://doi.org/10.2174/138945005774912735>.

48. THEISS, S. et al. Inactivation of the phospholipase B gene *PLB5* in wild-type *Candida albicans* reduces cell-associated phospholipase A2 activity and attenuates virulence. **International Journal of Medical Microbiology**, v. 296, n. 6, p. 405-420, 2006. DOI: <https://doi.org/10.1016/j.ijmm.2006.03.003>.
49. LEIDICH, S. D. et al. Cloning and disruption of *caPLB1*, a phospholipase B gene involved in the pathogenicity of *Candida albicans*. **The Journal of Biological Chemistry**, v. 273, n. 40, p. 26078-26086, 1998. DOI: <http://dx.doi.org/10.1074/jbc.273.40.26078>.
50. GHANNOUM, M. A. Potential role of phospholipases in virulence and fungal pathogenesis. **Clinical Microbiology Review**, v. 13, n. 1, p. 122-143, 2000.
51. FINKEL, J. S.; MITCHELL, A. P. Genetic of *Candida albicans* biofilm development. **Nature Reviews Microbiology**, v. 9, n. 2, p. 109-118, 2010. DOI: <https://doi.org/10.1038/nrmicro2475>.
52. UPPULURI, P. et al. Dispersion as an important step in the *Candida albicans* biofilm developmental cycle. **PLoS Pathogens**, v. 6, n. 3, e1000828, 2010. DOI: <https://doi.org/10.1371/journal.ppat.1000828>.
53. DOUGLAS, L. J. *Candida* biofilms and their role in infection. **Trends in Microbiology**, v. 11, n. 1, p. 30-36, 2003. DOI: [https://doi.org/10.1016/S0966-842X\(02\)00002-1](https://doi.org/10.1016/S0966-842X(02)00002-1).
54. KOJIC, E. M.; DAROUICHE, R. O. *Candida* infections of medical devices. **Clinical Microbiology Reviews**, v. 17, n. 2, p. 255-267, 2004. DOI: <https://doi.org/10.1128/CMR.17.2.255-267.2004>.
55. CHANDRA, J.; MUKHERJEE, P. K.; GHANNOUM, M. A. *Candida* biofilms associated with CVC and medical devices. **Mycoses**, v. 55, n. 1, p. 46-57, 2012. DOI: <https://doi.org/10.1111/j.1439-0507.2011.02149.x>.
56. ORTEGA, M. et al. *Candida* species bloodstream infection: epidemiology and outcome in a single institution from 1991 to 2008. **Journal of Hospital Infection**, v. 77, n. 2, p. 157-161, 2011. DOI: <https://doi.org/10.1016/j.jhin.2010.09.026>.
57. CHEN, C. Y. et al. Clinical characteristics of candidaemia in adults with haematological malignancy, and antimicrobial susceptibilities of the isolates at a medical centre in Taiwan, 2001–2010. **International Journal of Antimicrobial Agents**, v. 40, n. 6, p. 533-538, 2012. DOI: <https://doi.org/10.1016/j.ijantimicag.2012.07.022>.

58. KANG, S. J. et al. Clinical characteristics and risk factors for mortality in adult patients with persistent candidemia. **Journal of Infection**, v. 75, n. 3, p. 246-253, 2017. DOI: <https://doi.org/10.1016/j.jinf.2017.05.019>.
59. HAWSER, S. P.; DOUGLAS, L. J. Resistance of *Candida albicans* biofilms to antifungal agents *in vitro*. **Antimicrobial Agents and Chemotherapy**, v. 39, n. 9, p. 2128-2131, 1995. DOI: <https://doi.org/10.1128/AAC.39.9.2128>.
60. VEDIYAPPAN, G.; ROSSIGNOL, T.; d'ENFERT, C. Interaction of *Candida albicans* biofilms with antifungals: transcriptional response and binding of antifungals to beta-glucans. **Antimicrobial Agents and Chemotherapy**, v. 54, n. 5, p. 2096-2111, 2010. DOI: <https://doi.org/10.1128/AAC.01638-09>.
61. CAVALHEIRO, M.; TEIXEIRA, M. C. *Candida* biofilms: threats, challenges, and promising strategies. **Frontiers in Medicine**, v. 5, 2018. DOI: <https://doi.org/10.3389/fmed.2018.00028>.
62. GARCÍA-SÁNCHEZ, S. et al. *Candida albicans* biofilms: a developmental state associated with specific and stable gene expression patterns. **Eukaryotic Cell**, v. 3, n. 2, p. 536-545, 2004. DOI: <https://doi.org/10.1128/EC.3.2.536-545.2004>.
63. CHIN, V. K. et al. Dissecting *Candida albicans* infection from the perspective of *C. albicans* virulence and omics approaches on host–pathogen interaction: a review. **International Journal of Molecular Sciences**, v. 17, n. 10, p. 1643, 2016. DOI: <https://doi.org/10.3390/ijms17101643>.
64. AOKI, W. et al. Elucidation of potentially virulent factors of *Candida albicans* during serum adaptation by using quantitative time-course proteomics. **Journal of Proteomics**, v. 91, p. 417-429, 2013. DOI: <https://doi.org/10.1016/j.jprot.2013.07.031>.
65. BAGGERMAN, G. et al. Gel-based versus gel-free proteomics: a review. **Combinatorial Chemistry & High Throughput Screening**, v. 8, n. 8, p. 669-677, 2005. DOI: <https://doi.org/10.2174/138620705774962490>.
66. ABDALLAH, C. et al. Gel-based and gel-free quantitative proteomics approaches at a glance. **International Journal of Plant Genomics**, v. 2012, p.1-17, 2012. DOI: <http://dx.doi.org/10.1155/2012/494572>.

67. ASLAM, B. et al. Proteomics: technologies and their applications. **Journal of Chromatographic Science**, v. 55, n. 2, p. 182–196, 2017. DOI: <https://doi.org/10.1093/chromsci/bmw167>.
68. WALSH, G. M. et al. Mass spectrometry-based proteomics in biomedical research: emerging technologies and future strategies. **Expert Reviews in Molecular Medicine**, v. 12, e30, 2010. DOI: <https://doi.org/10.1017/S1462399410001614>.
69. MEGGER, D. A. et al. Label-free quantification in clinical proteomics. **Biochimica et Biophysica Acta (BBA) - Proteins and Proteomics**, v. 1834, n. 8, p. 1581-1590, 2013. DOI: <https://doi.org/10.1016/j.bbapap.2013.04.001>.
70. AL SHWEIKI, M. R. et al. Assessment of label-free quantification in discovery proteomics and impact of technological factors and natural variability of protein abundance. **Journal of Proteome Research**, v. 16, n. 4, p. 1410-1424, 2017. DOI: <https://doi.org/10.1021/acs.jproteome.6b00645>.

CHAPTER II

Manuscript 1 (Breaking report): “Serial systemic *Candida albicans* infection highlighted by proteomics”

Serial systemic *Candida albicans* infection highlighted by proteomics

Glaucia Sayuri Arita¹, Jean Eduardo Meneguello¹, Karina Mayumi Sakita¹, Daniella Renata Faria¹, Eduardo Jorge Pilau², Luciana Dias Ghiraldi-Lopes¹, Paula Aline Zanetti Campanerut-Sá¹, Érika Seki Kioshima¹, Patrícia de Souza Bonfim-Mendonça¹, Terezinha Inez Estivalet Svidzinski^{1*}

¹Department of Clinical Analysis and Biomedicine, State University of Maringá, Paraná, Brazil

²Department of Chemistry, State University of Maringá, Paraná, Brazil

*Corresponding author: Terezinha Inez Estivalet Svidzinski

Av. Colombo, 5790

ZIP CODE: 87020-900

Maringá, PR, Brazil

Phone: +55 44 3011-4809

Fax: +55 44 3011-4860

E-mail: terezinha.svidzinski@gmail.com

Abstract

Candida albicans is the major pathogen isolated from nosocomial bloodstream infections, leading to higher mortality rate. Thus, studies aiming to understand host-pathogen interactions are necessities. Therefore, we performed a murine model of serial systemic infection by *C. albicans* and we analyzed possible changes in the proteomic profiles. Firstly, we observed a reduction in the median survival time of infected animals among the passages, suggesting a higher pathogenicity acquired during repeated infections. By LC-MS/MS, it was possible to obtain protein profiles from wild-type strain (WT) and compare to proteins extracted from *Candida* cells recovered from infected tissues during the passages one, three and four (P1, P3 and P4). A total of 479 proteins were identified, with 56 proteins statistically significant in abundance in P1, 29 proteins in P3 and 97 proteins in P4. The proteins were categorized according to their potential role in virulence factors such as biofilm production, yeast-to-hyphae transition, phenotypic switching, proteins related to stress response and uncharacterized proteins. Therefore, with proteomic approach, it was possible to deepen the knowledge about host-pathogen interaction.

KEYWORDS

Candida albicans, systemic candidiasis, serial passage, virulence, host–pathogen interaction, proteomics, mass spectrometry, LC-MS/MS, label-free quantification

1 INTRODUCTION

Candida spp. are one of the most common agents of nosocomial bloodstream infections worldwide, leading to higher morbidity and mortality. Among them, *C. albicans* is still the major pathogen isolated (Lamoth, Lockhart, Berkow, & Calandra, 2018). Some of the main risk factors associated with candidemia are the use of antimicrobial agents, corticosteroid, chemotherapy, hematological malignancies, central venous catheter, gastrointestinal surgery, parenteral nutrition and an independent risk factor is hospitalization in the Intensive Care Unit (ICU) that facilitate dissemination of *Candida* among patients (Pfaller & Diekema, 2007). Risk of cross-transmission between healthcare workers' hands and ICU surfaces by strains with greater expression of virulence factors has also been previously described (Sakita et al., 2017).

Previous studies demonstrated that a model of serial infection provided insights into host-pathogen adaptations. Lüttich, Brunke, Hube, and Jacobsen (2013), after serial passages through the kidney, recovered strains with higher phenotypic variability; however, no overall virulence trend was observed. On the other hand, Cheng et al. (2007) recovered a mutant defective in the oxidative phosphorylation, but it was more resistant to phagocytosis and killing by neutrophils and macrophages after the fifth passage, demonstrating how *C. albicans* behaved during infection.

During interaction with the host, *C. albicans* faces to different pH, osmolarity, nutritional starvation and oxidative stress, then, responds to them by modifying its transcriptional profile to adapt to the surrounding environment (Calderone & Fonzi, 2001; Hube, 2004; Li et al., 2015). In the same way, protein profile also correlates with these changes, although some discrepancies between transcriptional and proteomic profiles exist (Lee et al., 2011). Therefore, proteomics is a valuable tool to understand adaptations that occurs in *C. albicans* to evade host defense and to invade tissues contributing to infection. Thus, this is the first study that aimed to use a proteomic view to elucidate host-pathogen interaction after serial systemic candidiasis in a murine model.

We found a reduction in the median survival time of the animals over the passages. The proteomic analysis provided insights how *C. albicans* interacted to the host by expressing proteins related to biofilm production, filamentation, phenotypic switching and stress response. These data contribute to the elucidation of how pathogen adapts to the host to cause infection enabling the investigation of possible targets of new therapeutic agents.

2 RESULTS AND DISCUSSION

2.1 Reduction of survival time after serial systemic candidiasis

The first step was to evaluate if serial infection, as represented in figure 1 a, could influence survival time in a murine model of systemic candidiasis. Then, we inoculated five mice per passage with 3.5×10^5 *C. albicans* cells and followed up until their death. In figure 1b, a decreasing trend in the median survival time was observed in animals infected with colonies recovered ($p < .0002$ in log-rank test) in a successive way. After adjusting significance for multiple comparisons between each passage to control, the median survival time for the animals infected with the wild type strain (WT) and P1 was 10 days, and seven days for P2 ($p = .3728$ and $p = .0472$, respectively). From P3 onwards, a significant reduction of median survival time in relation to WT was observed ($p = .0031$ (P3), $p = .0019$ (P4) and $p = .0035$ (P5)).

In general, all animals infected lost their body weight; furthermore, they became severely ill after third passage that coincides with reduced survival time. The group of animals infected by WT lost 29% of their body weight. Similarly, groups infected by P1 lost 22% of weight; by P2, the loss weight was 29%; P3 and P4 lost 24%. Lastly, animals infected by P5 lost 25% of weight. In contrast, healthy mice (without infection; WI) were followed up throughout the experiment and they presented a gain weight of approximately 6%. During serial infection, animals presented abdominal contortion and piloerection, and these behavioral parameters were more evident in mice infected by P3 to P5; this fact is possibly related to shorter survival times.

Once *C. albicans* enters the bloodstream, it can invade many organs and will find different conditions (pH, levels of oxygen and carbon dioxide, nutrients) that will induce *Candida* cells to adapt and cause disease (Calderone & Fonzi, 2001; Hube, 2004; Li et al., 2015). In addition, *C. albicans* express virulence factors that will contribute to pathogenicity.

Therefore, the lost weight summed up with worse behavioral parameters and reduced survival time provide insights about pathogenicity of *C. albicans* acquired during repeated infections.

2.2 Proteomics profile after serial infection reveals proteins related to virulence factors

Disseminated systemic candidiasis is related to two main factors: host susceptibility and/or increased fungal virulence during the infectious process (Calderone & Fonzi, 2001; Pfaller & Diekema, 2007). Once we work with healthy animals, our results in the reduction of

survival time suggest the hypothesis that after the serial contact with host, there was an increased virulence in yeasts. Therefore, we used proteomic view to evaluate the protein profile in the most prominent passages (P1, P3 and P4). Proteome analysis is an important approach for comprehensive characterization of dynamic variations that occur during adaptation of microorganisms under different conditions. Considering that the metabolic study of microorganism is complex, this technical provides the opportunity to identify proteins that may be targets in the *C. albicans* pathogenicity (Lee et al, 2011; Aoki 2013b). To the best of our knowledge, this is the first study to assess proteomic profile of the *C. albicans* after serial passage in a systemic candidiasis model.

Therefore, we selected three passages for proteomic analysis plus WT. Then, we chose P1 because it is the beginning of serial infection and also P3 and P4 because of the significant reduction in survival time. A total of 479 proteins were identified and all proteins from passages were compared in their abundance in relation to WT (Supplemental data). Thus, a Venn diagram was constructed and showed 13 proteins were shared with all passages (Figure 2 a). From 56 proteins differentially in abundance in P1, 15 were in common to P4. From 29 proteins that were differentially in abundance in P3, seven were in common to P4. The unique proteins that were significantly different only in one passage compared to WT were 28, 9 and 62 proteins for P1, P3 and P4, respectively. The remaining proteins were not significantly different in any passages in relation to WT.

We further classified proteins according to their biological processes and divided them in lower in abundance (green bar) and higher in abundance (red bar) for P1, P3 and P4 (Figure 2 b-d). The majority of proteins were related to carbohydrate metabolism in all passages, followed by stress response proteins and amino acid metabolism. We also found proteins involved in protein biosynthesis/folding, lipid metabolism, metabolism of cofactors and vitamins, glyoxylate cycle and energy metabolism during all passages. Proteins related to mitochondrial biogenesis were found only in P4. Furthermore, from 56 proteins in P1, 35 proteins were in increased in abundance and 21 decreased in abundance than WT. From 29 proteins in P3, 12 were higher in abundance and 17 lower in abundance when compared to WT. In the same way, from 97 proteins in P4, 41 were increased in abundance and 56 were decreased in abundance than WT. It can be observed a more active metabolism with proteins from amino acid and carbohydrate metabolism increased in abundance in P1 when compared to the remaining passages, as seen in P3 that exhibited only proteins decreased in abundance. This

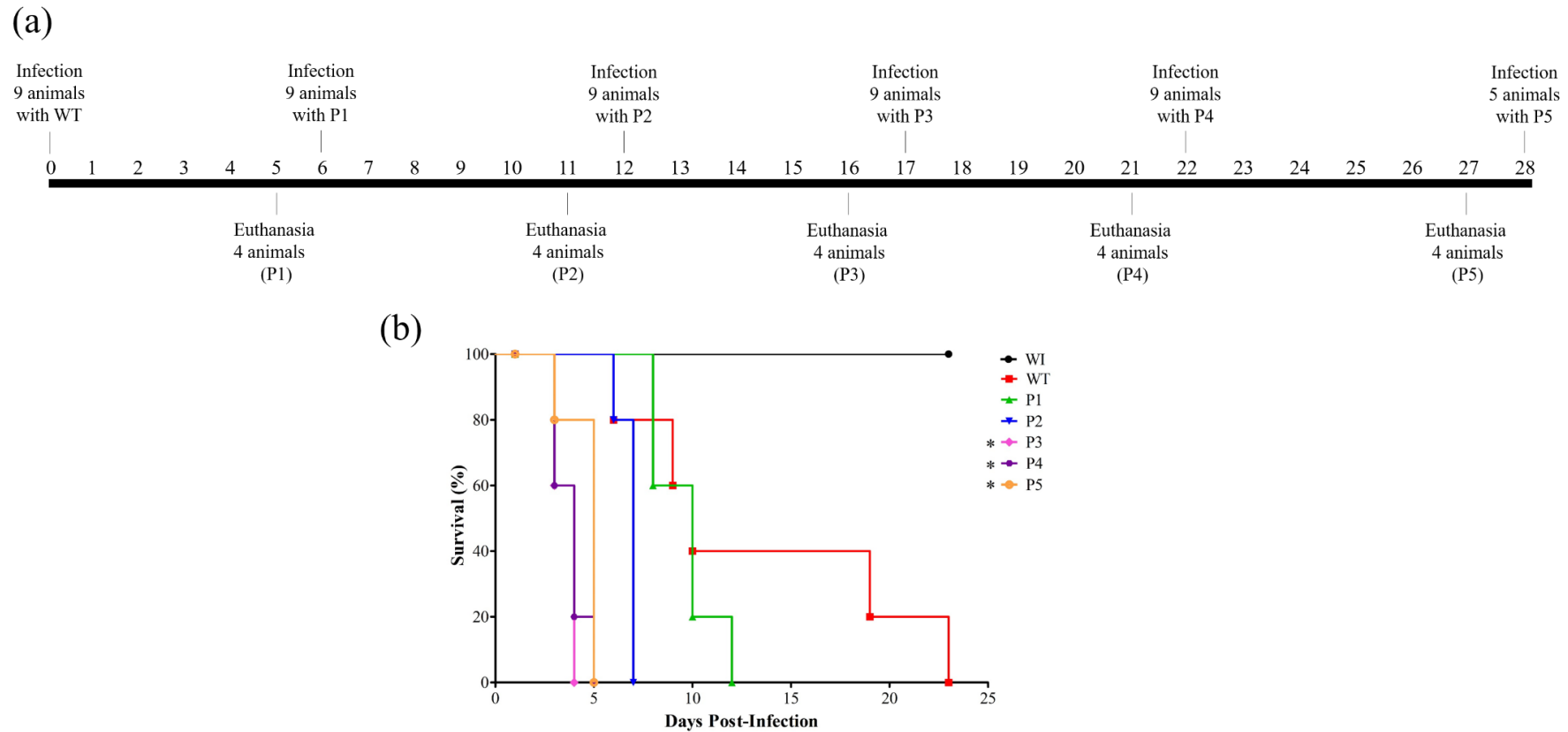


FIGURE 1 Model of serial systemic candidiasis reduces survival time of animals infected by yeasts recovered from passages. (a) Serial infection timeline starting with nine mice being infected by wild-type *C. albicans* SC5314 strain (WT) at day zero, followed by euthanasia of four animals at day five to recover their colonies to use for inoculum preparation to infect nine animals for the next passage. The remaining five animals were used for survival curve. Timeline was designed from passage 1 to 5 (P1-P5). (b) Survival curve from group of five animals each infected by 3.5×10^5 cells of *C. albicans* and monitored until their natural death. In addition, healthy mice (without infection; WI) were also followed up. This survival curve represents at least two independent experiments. Log-rank test for multiple comparisons between each passage to control was applied; $*p = .0031$ (P3), $*p = .0019$ (P4) and $*p = .0035$ (P5).

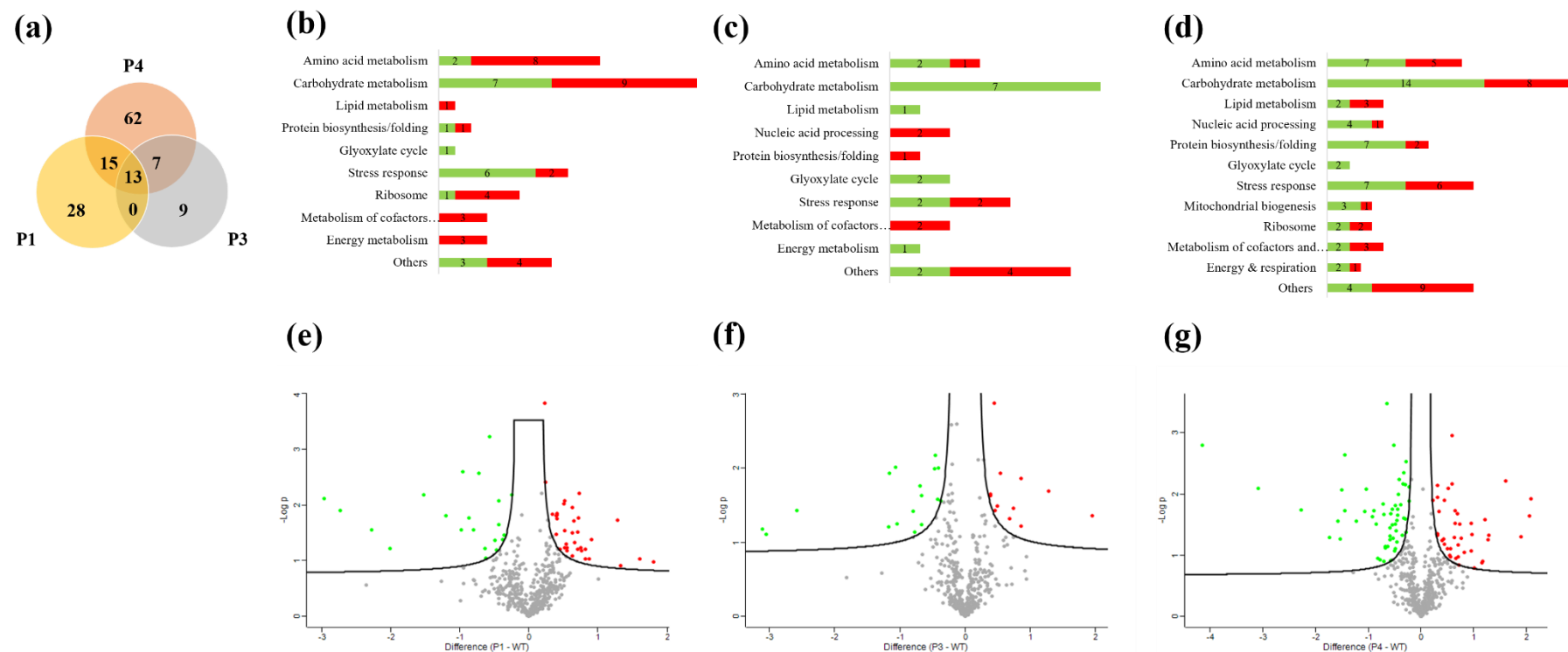


FIGURE 2 Proteomic analysis from *Candida albicans* recovered from serial systemic infection. (a) Venn diagram showing proteins from each passage: 13 proteins are common to all evaluated passages (P1, P3 and P4), 15 proteins common to P1 and P4, 7 proteins common to P3 and P4. The unshared part represents unique proteins: 28, 9 and 62 proteins for P1, P3 and P4, respectively. (b-d) Proteins were classified according to their biological process and divided between lower abundance (green bar) and higher abundance (red bar) for P1, P3 and P4. (e-f) Volcano plot represents graphically the data from negative logarithmic p -values of the t -test against difference of the protein intensities between passages and wild type strain. Proteins decreased in abundance (green dots), increased in abundance (red dots) and without significant differences (grey dots).

fact could be possibly related to adaptation of the pathogen in the host and to expression of virulence attributes.

A volcano plot was constructed by plotting in y-axis, logarithmic ratios of the protein intensities and in x-axis, negative logarithmic p-values of the t-test performed from biological duplicate experiments. Proteins increased in abundance in the passages (red dots), decreased in abundance in the passages (green dots) and without significant differences (grey dots) (Figure 2 e-g).

Gathering the knowledge about the early death of the animals after the serial passages in a systemic candidiasis model, associated with the findings of differentially expressed proteins, we added efforts to understand the protein profile directly linked to the pathogenicity of *C. albicans*. Then, we searched in the literature for proteins or genes whose expression increases or reduces associated with virulence factors in *C. albicans*. Therefore, we categorized proteins found in our study in relation to their role in virulence factors such as biofilm, filamentation, phenotypic switching, stress response and other (Table 1).

We found several proteins related to biofilm, among them, cystathionine gamma-lyase (Cys3), a protein from amino acids metabolism, was higher in abundance in all passages than in the WT. In contrast, malate synthase (Mls1), which is a key glyoxylate cycle enzyme, was decreased in abundance in all passages. García-Sánchez et al. (2004) described that genes involved in synthesis of sulfur amino acids were overexpressed in biofilm and genes related to glucose repression such as *MLS1* were underexpressed, corroborating with our results. Another protein presented in all passages was yeast-form wall protein 1 (Ywp1), a glycoprotein of the yeast form cell wall, literature reports strain lacking Ywp1 presents higher adhesivity and biofilm formation. In this way, the elevated abundance of Ywp1 in the three passages compared to WT implies lower adhesiveness and could be related to better ability to disseminate during infection in the host (Gow, Brown, & Odds, 2002; Granger, Flenniken, Davis, Mitchell, & Cutler, 2005). All of other proteins (Cef3, Mir1, Ifd6, Adh1, Cdc19, Rhr2, Mpg1) related to biofilm were higher in abundance in the passages than in WT which is in agreement with literature (Desai et al., 2015; Marchias et al., 2005; Thomas, Bachmann, & Lopez-Ribot, 2006; Ying et al., 2010). It should be noted that P1 and P4 presented more proteins with significantly difference in abundance than P3.

Regarding proteins related to yeast-to-hyphae transition, Rashki, Ghalehnoo, and Dominguez (2012) conducted a study of genes expressed during early stage of filamentation.

Interesting, we found proteins from box C/D snoRNO complex (Nop1, Nop58 and Sik1) increased in abundance in P1 and their genes were upregulated during early phase of filamentation, confirming involvement of ribosome biogenesis during infection, in P1 particularly (Rashki et al., 2012). Aoki et al. (2013a) identified 16 unique proteins expressed during transition to hypha in the entire period studied, as glycerol 3-phosphatase (Rhr2) which is present only in P4, reflecting a possible role in filamentation during this passage. The same group performed quantitative time-course proteomics from *C. albicans* during filamentation in fetal bovine serum (FBS) and found a protein named Blood-induced peptide 1 (Blp1) that showed tolerance to various stress conditions, revealing its potential role as a virulence factor (Aoki et al., 2013b). Thus, its significant abundance in P4 might reflect acquired tolerance after serial passaging. Furthermore, the presence of Cys3 in all passages, which is involved at sulphur metabolism, also contributed to yeast-to-hypha transition according to Rashki et al. (2012). These authors also found genes that were upregulated (*TIF34* and *TIM9*) and some were downregulated (*ACH1*, *CIT1*, *SOD1*, *IFE2*, *AAT21*, *MDH1*, *GDH3* and *GSY1*) which can be correlated with our proteomic findings. Therefore, the presence of proteins related to filamentation suggests that transition to hyphae form could have contributed to the reduction in survival time of the animals over the passages.

We found proteins that indicate the process of phenotypic switching in our passages that are important to yeast-to-hyphae transition. We found increased in abundance of fumarate reductase (Osm2) in P1 and P4. According to Si, Hernday, Hirakawa, Johnson & Bennett, 2013, *OSM2* gene was induced only in opaque filaments, although white type has shown to be more virulent in systemic models. Furthermore, levels of CO₂ induced white-to-opaque switch, downregulating white-specific genes such as *WH11* and *EFG1* and upregulating opaque-specific genes such as *OP4* and *WOR1*, which are important for mating (Huang, Srikantha, Sahni, Yi, & Soll, 2009). Thus, decreased in abundance of Wh11p found in P3 would imply a possible role in virulence for opaque type as well.

Superoxide dismutase 1 and 3 (SOD1 and SOD3) were increased in abundance in all the three passages. *C. albicans* has six different superoxide dismutase enzymes. Among them, SOD1 is a cytosolic dependent of copper-zinc (Cu/Zn) as cofactor and SOD3 is dependent of manganese (Mn). Under Cu starvation conditions, as during *C. albicans* systemic infection in kidney, there is a switch expression of SOD1 to SOD3 controlled by the Cu-sensing regulator

Mac1 (Chauhan, Latge, & Calderone, 2006; Li et al., 2015). This finding is in according to our results, denoting low concentrations of Cu during systemic infection.

Host defense can be exercised by macrophages producing reactive oxygen and nitrogen species (Vázquez-Torres & Balish, 1997). Thus, exposure to nitric oxide (NO) has already been shown to induce expression of *YHB1* and *DDR48* in *C. albicans* (Hromatka, Noble & Johnson, 2005). These findings are correlated to increased in abundance in the respective proteins flavohemoprotein (Yhb1) and Stress protein DDR48 (Ddr48p) during passages. Moreover, *DDR48* has already been described to have a critical role during filamentation and virulence although it is not a consensus in the literature (Dib, Hayek, Sadek, Beyrouthy, & Khalaf, 2008; Cleary, MacGregor, Saville, & Thomas, 2012).

We also found some proteins that have not been characterized yet, as orf19.36.1. It is decreased in abundance in P1 but increased in abundance in P4; therefore, this protein could be a virulence factor that should be investigated in next studies, since P4 was related to a reduced animal survival time in the murine model of systemic candidiasis and exhibited more proteins associated with stress response.

Altogether, our results demonstrated a significant reduction in the median survival time over the passages. Expression of proteins related to virulence factors might have influenced the increased pathogenicity observed. In this way, phenotypic assays highlighted by proteomics findings should be performed and then, to deepen the study of these proteins aiming their role as virulence markers and therapeutic targets.

TABLE 1 Proteins categorized according to their role in virulence factors

	Gene	Protein	P1xWT	P3xWT	P4xWT	Literature
Biofilm	<i>CYS3</i>	Cystathionine gamma-lyase	0.8688	0.6811	0.9481	García-Sánchez et al. (2004)
	<i>YWPI</i>	Yeast-form wall Protein 1	0.5545	1.2769	1.6142	Gow et al. (2002); Granger et al. (2005)
	<i>CEF3/EFT3</i>	Elongation factor 3	0.4013	-	-	Marchias et al. (2005)
	<i>MIR1</i>	Mir1p	0.4497	-	-	Marchias et al. (2005)
	<i>IFD6</i>	Ifd6p	1.2875			Ying et al. (2010)
	<i>ADH1</i>	Adh1p	-	-	0.8220	Thomas et al. (2006)
	<i>CDC19</i>	Pyruvate kinase	-	-	0.5644	Thomas et al. (2006)

	<i>RHR2</i>	Glycerol-1-phosphatase	-	-	0.7219	Desai et al. (2015)
	<i>MPG1</i>	Mannose-1-phosphate guanylyltransferase	-	-	0.3982	Marchias et al. (2005)
	<i>MLS1</i>	Malate synthase	-2.7376	-3.0497	-3.0866	García-Sánchez et al. (2004)
Filamentation	<i>CYS3</i>	Cystathionine gamma-lyase	0.8688	0.6811	0.9481	Rashki et al. (2012)
	<i>NOPI</i>	rRNA methyltransferase	0.4075	-	-	Rashki et al. (2012)
	<i>NOP58</i>	Nucleolar protein 58	0.3969	-	-	Rashki et al. (2012)
	<i>SIK1</i>	snoRNP complex protein	0.2416	-	-0.2836	Rashki et al. (2012)
	<i>TIF34</i>	Eukaryotic translation initiation factor 3 subunit I	-	0.4610	-	Rashki et al. (2012)
	<i>DDR48</i>	Stress protein DDR48	-	-	1.2947	Dib et al. (2008); Cleary et al. (2012)
	<i>RHR2</i>	Glycerol-1-phosphatase	-	-	0.7219	Aoki et al. (2013a)
	<i>ACH1</i>	Acetyl-CoA hydrolase	-0.7261	-0.6624	-1.0314	Rashki et al. (2012)
	<i>CIT1</i>	Citrate synthase	-0.8699	-1.0656	-1.2239	Rashki et al. (2012)
	<i>SOD1</i>	Superoxide dismutase [Cu-Zn]	-2.2817	-2.5826	-1.7312	Rashki et al. (2012)
	<i>IFE2</i>	Ife2p	-1.2083	-1.0490	-1.4998	Rashki et al. (2012)
	<i>AAT21</i>	Aspartate aminotransferase	-0.5720	-	-0.5414	Rashki et al. (2012)
	<i>MDH1</i>	Malate dehydrogenase, cytoplasmic	-2.0160	-	-1.5697	Rashki et al. (2012)
	<i>GDH3</i>	Glutamate dehydrogenase	-	-0.6970	-	Rashki et al. (2012)
	<i>GSY1</i>	Glycogen [starch] synthase	-	-	-0.2303	Rashki et al. (2012)
Phenotypic switching	<i>OSM2</i>	Fumarate reductase	0.7646	-	0.5936	Si et al. (2013)
	<i>WH11</i>	Wh11p	-	-0.8011	-	Huang et al. (2009)

Stress response	<i>SOD1</i>	Superoxide dismutase [Cu-Zn]	-2.2817	-2.5826	-1.7312	Chauhan et al. (2006); Li et al. (2015)
	<i>SOD3</i>	Superoxide dismutase	1.6093	1.9415	2.0571	Rashki et al. (2012)
	<i>YHBI</i>	Flavoheмоprotein	0.6299	0.5347	0.3077	Hromatka et al. (2005)
	<i>BLP1</i>	Blood-induced peptide 1	-	-	1.2168	Aoki et al. (2013b)
Other	orf19.36.1	Uncharacterized	-0.6240	-	1.8996	Uncharacterized

3 EXPERIMENTAL PROCEDURES

3.1 Ethics statement

All procedures were approved by the Ethics Committee for Animal Use of the State University of Maringá, PR, Brazil under the protocol number CEUA 7261020418 which is in accordance with the Brazil's National Council for the Control of Animal Experimentation (CONCEA).

3.2 Strain and culture conditions

Reference strain *C. albicans* SC5314 was used for the initial infection in a murine model of disseminated candidiasis. First, it was cultured on Sabouraud Dextrose Broth (Difco). Next, a loop was streaked on CHROMagar™ *Candida* (Becton Dickinson). Then, a single colony was streaked on Sabouraud Dextrose Agar (SDA) (Difco) plate and incubated for 24 h at 35 °C. An inoculum of 3.5×10^5 cells was prepared in Phosphate Buffered Saline (PBS, pH 7.4).

3.3 Murine model of serial disseminated candidiasis and survival curve

Considering that mice death are not homogenous; then, in order to obtain a standardization in the passages, we selected for each passage one group of five animals for survival curve experiment and monitored until their natural death and one group of four animals that were humanely euthanized to use the colonies recovered to prepare the inoculum for the next passage (Figure 1).

The serial systemic candidiasis consisted of initially infect nine female Balb/c mice by wild-type *C. albicans* SC5314 (WT) with 0.1 ml of prepared inoculum via lateral tail vein. The

group of five animals of survival curve experiment was monitored through their behavior parameters, weighted daily, and followed up until their natural death. Then, five days post-infection, the group of four animals was humanely euthanized. The kidney was aseptically removed, homogenized in lysis buffer (200 mM NaCl, 5 mM EDTA, 10 mM Tris, 10% glycerol v/v, pH 8.30), plated on SDA and incubated for 24 h at 35 °C. Colonies recovered from infected kidney were used to prepare inoculum for the subsequent infections as described for WT, totalizing five serial passages (P1-P5). Healthy animals (without infection) were humanely terminated at the end of the experiment and were used as reference in the survival curve and for monitoring the weight of animals.

3.4 Proteomics

For proteome analysis, *Candida* cells recovered from kidney and plated on SDA were collected and centrifuged for 5 min for 3000 rpm. The pellet was washed three times with ultrapure water and resuspended in 1100 µL of buffer containing 7 M urea, 2 M thiourea, and 40 mM DTT (Fiorini et al., 2016). Then, the suspension was sonicated (30 bursts of 10 seconds ON, 30 seconds OFF with 100% amplitude). After that, the lysate was centrifuged at 4800 rpm for 10 min at 4 °C, and supernatant collected and stored at -80 °C. Bradford assay was performed for protein quantification, using bovine serum albumin (Sigma) as a standard. Prior to digestion, protein content was denatured with 8M urea, then, reduced with 5 mM dithiothreitol (DTT) and alkylated with 14 mM iodoacetamide (IAA). For the quench of the remaining IAA, 5 mM DTT was added. Samples were diluted with four volumes of 50 mM ammonium bicarbonate and 1 mM calcium chloride was added with subsequent trypsin (V5280 - Promega) digestion at 37 °C overnight (ratio of 1 µg enzyme to 100 µg protein). Then, samples were acidified with 0.4% trifluoroacetic acid to stop trypsin action and desalted using SepPak tC18 cartridges (WAT 036820).

Samples were analyzed by LC-MS/MS using ultra-high performance liquid chromatography (Shimadzu, Nexera X2, Japan) coupled to high resolution mass spectrometry (Impact II, Bruker Daltonics Corporation, Germany) and equipped with an electrospray ionization source. Ten microliter of the sample were loaded at flow of 0.1000 ml/min. The capillary voltage was operated in positive ionization mode, set at 4500 V and with an end plate offset potential of -500 V. The dry gas parameters were set to 7.0 L min⁻¹ at 180 °C with a nebulization gas pressure of 2.0 bar. Data were collected from m/z 150-2200 with an acquisition

rate of 5 spectrums per second, and the ions of interest were selected by auto MS/MS scan fragmentation. Chromatographic separation was performed using gradient A containing purified water and 0.1% formic acid (v/v) and B containing acetonitrile with 0.1% formic acid (v/v) using a C18 column (Shim-pack GIST - 3 μ m x 1.0 mm x 250 mm). The gradient used was 2%, 35%, 95%, 95% and 2% of B in 2, 60, 90, 110 and 111 min respectively, and stopped at 120 min.

Files obtained by the mass spectrometer were normalized using Data Analysis software (Bruker, Germany), converted in a vendor free file by MSFile from the ProteoWizard Platform (Chambers et al., 2012) and processed in MaxQuant software (version 1.6.2.3) (Tyanova et al., 2015) for label free quantification (LFQ). The proteins were searched against reference proteome from *C. albicans* (strain SC5314 / ATCC MYA-2876) taxonomy code 237561 from UniProt Database. Parameters were set for digestion mode specific for trypsin with maximum of two missed cleavage sites. Variable modifications were oxidation (M) and acetyl (Protein N-term) and fixed modification was carbamidomethyl (C) with maximum of five modifications. False discovery rate (FDR) were set to 0.01 for both peptide and protein levels. Then, MaxQuant output file was imported in Perseus (version 1.6.1.3) (Tyanova et al., 2016) for statistical analysis. First, protein dataset were filtered, removing proteins into categorical parameters: contaminant, only identified by site and reverse database. For statistical analysis, the level of stringency was set protein identification with LFQ values greater than zero in two of the replicates. Thus, data analysis was performed using two sample test, considering significant those proteins with $-\log_{10}(p \text{ value}) < .05$ associated with the highest difference (passage *versus* WT).

All proteins were classified according to molecular functions and/or biological processes obtained from UniProt (<https://www.uniprot.org/>) and *Candida* Genome Database (<http://www.candidagenome.org/>). Furthermore, proteins were separated according to their role in virulence factors expressed in *C. albicans*.

3.5 Statistical analysis

Survival curve data were analyzed by GraphPad Prism version 6.00 for Windows (GraphPad Software, San Diego, CA, USA). Thus, two groups were compared at a time, being each passage with control, so the significance was adjusted to account for multiple comparisons.

In this way, log-rank (Mantel-Cox) test were used and *p value* lower than 0.01 were considered statistically significant.

ACKNOWLEDGEMENTS

We thank Coordenação de Aperfeiçoamento de Pessoal de Nível Superior (CAPES), Conselho Nacional de Desenvolvimento Científico e Tecnológico (CNPq) and Fundação Araucária for the financial support.

CONFLICT OF INTEREST

The authors declare there was no conflict of interest.

AUTHOR CONTRIBUTION

G.S.A, K.M.S and D.R.F., performed the experiments with animals; G.S.A. and J.E.M performed the proteomics experiments; All authors analyzed the data and G.S.A., P.S.B.M and T.I.E.S. wrote the paper.

REFERENCES

- Aoki, W., Ueda, T., Tatsukami, Y., Kitahara, N., Morisaka, H., Kuroda, K., & Ueda, M. (2013a). Time-course proteomic profile of *Candida albicans* during adaptation to a fetal serum. *Pathogens and Disease*, 67(1), 67-75. <https://doi.org/10.1111/2049-632X.12003>.
- Aoki, W., Tatsukami, Y., Kitahara, N., Matsui, K., Morisaka, H., Kuroda, K., & Ueda, M. (2013b). Elucidation of potentially virulent factors of *Candida albicans* during serum adaptation by using quantitative time-course proteomics. *Journal of Proteomics*, 91, 417-429. <https://doi.org/10.1016/j.jprot.2013.07.031>.
- Calderone, R. A., Fonzi, W. A. (2001). Virulence factors of *Candida albicans*. *Trends in Microbiology*, 9(7), 327-335.
- Chambers, M. C., Maclean, B., Burke, R., Amodei, D., Ruderman, D. L., Neumann, S., ... Mallick, P. (2012). A cross-platform toolkit for mass spectrometry and proteomics. *Nature Biotechnology*, 30(10), 918-920. <https://doi.org/10.1038/nbt.2377>.
- Chauhan N., Latge, J. P., & Calderone, R. (2006). Signalling and oxidant adaptation in *Candida albicans* and *Aspergillus fumigatus*. *Nature Reviews Microbiology*, 4, 435-444. <https://doi.org/10.1038/nrmicro1426>.

- Cheng, S., Clancy, C. J., Zhang, Z., Hao, B., Wang, W., Iczkowski, K. A., ... Nguyen, M. H. (2007). Uncoupling of oxidative phosphorylation enables *Candida albicans* to resist killing by phagocytes and persist in tissue. *Cellular Microbiology*, 9(2), 492-502.
- Cleary, I. A., MacGregor, N. B., Saville, S. P., & Thomas, D. P. (2012). Investigating the function of Ddr48p in *Candida albicans*. *Eukaryotic Cell*, 11(6), 718-724. <https://doi.org/10.1128/EC.00107-12>.
- Desai, J. V., Cheng, S., Ying, T., Nguyen, M. H., Clancy, C. J., Lanni, F., & Mitchell, A. P. (2015). Coordination of *Candida albicans* invasion and infection functions by phosphoglycerol phosphatase Rhr2. *Pathogens*, 4, 573-589. <https://doi.org/10.3390/pathogens4030573>.
- Dib, L., Hayek, P., Sadek, H., Beyrouthy, B., & Khalaf, R. A. (2008). The *Candida albicans* Ddr48 protein is essential for filamentation, stress response, and confers partial antifungal drug resistance. *Medical Science Monitor*, 14(6), BR113-121.
- Fiorini, A., Rosado, F. R., Bettiga, E. M. S., Melo, K. C. S., Kukolj, C., Bonfim-Mendonça, P. S., ... Svidzinski, T. I. E. (2016). *Candida albicans* protein profile changes in response to the butanolic extract of *Sapindus saponaria* L. *Revista do Instituto de Medicina Tropical de São Paulo*, 58, 25. <http://dx.doi.org/10.1590/s1678-9946201658025>.
- García-Sánchez, S., Aubert, S., Iraqui, I., Janbon, G., Ghigo, JM., & d'Enfert, C. (2004). *Candida albicans* biofilms: a developmental state associated with specific and stable gene expression patterns. *Eukaryotic Cell*, 3, 536-545. <https://doi.org/10.1128/EC.3.2.536-545.2004>.
- Gow, N. A., Brown, A. J. P., & Odds, F. C. (2002). Fungal morphogenesis and host invasion. *Current Opinion in Microbiology*, 5(4), 366-371. [https://doi.org/10.1016/S1369-5274\(02\)00338-7](https://doi.org/10.1016/S1369-5274(02)00338-7).
- Granger, B. L., Flenniken, M. L., Davis, D. A., Mitchell, A. P., & Cutler, J. E. (2005). Yeast wall protein 1 of *Candida albicans*. *Microbiology*, 151(5), 1631-1644. <https://dx.doi.org/10.1099/mic.0.27663-0>.
- Hromatka, B. S., Noble, S. M., & Johnson, A. D. (2005). Transcriptional response of *Candida albicans* to nitric oxide and the role of the *YHB1* gene in nitrosative stress and virulence. *Molecular Biology of the Cell*, 16(10), 4814-4826.
- Huang, G., Srikantha, T., Sahni, N., Yi, S., & Soll, D. R. (2009). CO₂ regulates white-to-opaque switching in *Candida albicans*. *Current Biology*, 19(4), 330-334. <https://doi.org/10.1016/j.cub.2009.01.018>.
- Hube, B. (2004). From commensal to pathogen: stage- and tissue-specific gene expression of *Candida albicans*. *Current Opinion in Microbiology*, 7(4), 336-341.

- Lamoth, F., Lockhart, S. R., Berkow, E., & Calandra, T. (2018). Changes in the epidemiological landscape of invasive candidiasis. *Journal of Antimicrobial Chemotherapy*, 73(1), i4-i13. <https://doi.org/10.1093/jac/dkx444>.
- Lee, M. V., Topper, S. E., Hubler, S. L., Hose, J., Wenger, C. D., Coon, J. J., & Gasch, A. P. (2011). A dynamic model of proteome changes reveals new roles for transcript alteration in yeast. *Molecular Systems Biology*, 7, 514. <https://doi.org/10.1038/msb.2011.48>.
- Li, C. X., Gleason, J. E., Zhang, S. X., Bruno, V. M., Cormack, B. P., & Culotta, V. C. (2015). *Candida albicans* adapts to host copper during infection by swapping metal cofactors for superoxide dismutase. *Proceedings of the National Academy of Sciences of the United States of America*, 112(38), E5336-E5342. <https://doi.org/10.1073/pnas.1513447112>.
- Lüttich, A., Brunke, S., Hube, B., & Jacobsen, I. D. (2013). Serial passaging of *Candida albicans* in systemic murine infection suggests that the wild type strain SC5314 is well adapted to the murine kidney. *PLoS ONE*, 8(5), e64482. <https://doi.org/10.1371/journal.pone.0064482>.
- Marchais, V., Kempf, M., Licznar, P., Lefrançois, C., Bouchara, JP., Robert, R., & Cottin, J. (2005). DNA array analysis of *Candida albicans* gene expression in response to adherence to polystyrene. *FEMS Microbiology Letters*, 245, 25-32. <https://doi.org/10.1016/j.femsle.2005.02.014>.
- Pfaller, M. A., & Diekema, D. J. (2007). Epidemiology of invasive candidiasis: a persistent public health problem. *Clinical Microbiology Reviews*, 20(1), 133-163. <https://doi.org/10.1128/CMR.00029-06>.
- Rashki A., Ghalehnoo, Z. R., & Dominguez, R. (2012). The early response of *Candida albicans* filament induction is coupled with wholesale expression of the translation machinery. *Comparative Clinical Pathology*, 21(6), 1533-1545. <https://doi.org/10.1007/s00580-011-1325-1>.
- Sakita, K. M., Faria, D. R., Silva, E. M. D., Tobaldini-Valério, F. K., Kioshima, E. S., Svidzinski, T. I. E., & Bonfim-Mendonça, P. S. (2017). Healthcare workers' hands as a vehicle for the transmission of virulent strains of *Candida* spp.: a virulence factor approach. *Microbial Pathogenesis*, 113, 225-232. <https://doi.org/10.1016/j.micpath.2017.10.044>.
- Si, H., Hernday, A. D., Hirakawa, M. P., Johnson, A. D., & Bennett, R. J. (2013). *Candida albicans* white and opaque cells undergo distinct programs of filamentous growth. *PLoS Pathogens*, 9(3), e1003210. <https://doi.org/10.1371/journal.ppat.1003210>.
- Thomas, D. P., Bachmann, S. P., & Lopez-Ribot, J. L. (2006). Proteomics for the analysis of the *Candida albicans* biofilm lifestyle. *Proteomics*, 6, 5795-5904. <https://doi.org/10.1002/pmic.200600332>.

- Tyanova, S., Temu, T., Carlson, A., Sinitcyn, P., Mann, M., & Cox, J. (2015). Visualization of LC-MS/MS proteomics data in MaxQuant. *Proteomics*, 15, 1453–1456. <https://doi.org/10.1002/pmic.201400449>.
- Tyanova, S., Temu, T., Sinitcyn, P., Carlson, A., Hein, M. Y., Geiger, T., ... Cox, J. (2016). The Perseus computational platform for comprehensive analysis of (prote)omics data. *Nature Methods*, 13(9), 731–740. <https://doi.org/10.1038/nmeth.3901>.
- Vázquez-Torres, A., & Balish, E. (1997). Macrophages in resistance to candidiasis. *Microbiology and Molecular Biology Reviews*, 61(2), 170-192.
- Ying, L., DeDong, L., Yan, W., LingCong, L., Hai, H., ShouTing, F., & YuanYing J. (2010). Overexpression of *IFD6* in *Candida albicans* promotes biofilm formation [Abstract]. *Academic Journal of Second Military Medical University*, 31(6), 599-603.

Supplemental data

Table S1. Identification of proteins from *Candida albicans* (Passage 1) by mass spectrometry

Protein IDs	Gene name	UniProt names	Molecular function	Biological process	*Difference
Amino acid metabolism					
A0A1D8PG20	<i>ARO8</i>	Bifunctional 2-aminoadipate transaminase/aromatic-amino-acid:2-oxoglutarate transaminase	2-aminoadipate transaminase activity; aromatic-amino-acid:2-oxoglutarate aminotransferase activity e pyridoxal phosphate binding	aromatic amino acid family biosynthetic process; aromatic amino acid family catabolic process; aromatic amino acid family catabolic process to alcohol via Ehrlich pathway; L-lysine catabolic process; lysine biosynthetic process via amino adipic acid	0.5215501785
A0A1D8PIB2	<i>ASN1</i>	Asparagine synthase (Glutamine-hydrolyzing) 2	asparagine synthase (glutamine-hydrolyzing) activity; ATP binding	asparagine biosynthetic process; glutamine metabolic process	0.713186264
A0A1D8PKB9	<i>BAT22</i>	Branched-chain-amino-acid aminotransferase	L-isoleucine transaminase activity; L-leucine transaminase activity; L-valine transaminase activity	branched-chain amino acid biosynthetic process	0.6488876343
Q59N40	<i>AAT21</i>	Aspartate aminotransferase	L-aspartate:2-oxoglutarate aminotransferase activity; pyridoxal phosphate binding	biosynthetic process; cellular amino acid metabolic process	-0.5720386505
Q59R18	<i>DED81</i>	Asparagine--tRNA ligase	asparagine-tRNA ligase activity; ATP binding; nucleic acid binding	asparaginyl-tRNA aminoacylation	0.819188118
Q59R20	orf19.6701	Proline--tRNA ligase	aminoacyl-tRNA editing activity; ATP binding; proline-tRNA ligase activity	prolyl-tRNA aminoacylation	0.4004220963
Q59RI1	<i>ILS1</i>	Proline--tRNA ligase	aminoacyl-tRNA editing activity; ATP binding; isoleucine-tRNA ligase activity; tRNA binding	isoleucyl-tRNA aminoacylation	0.3450279236
Q5A362	<i>CYS3</i>	Cystathionine gamma-lyase	cystathionine gamma-lyase activity; pyridoxal phosphate binding	cysteine biosynthetic process via cystathionine; methionine biosynthetic process; transsulfuration	0.8688545227

Q5AKX1	<i>GCV3</i>	Glycine cleavage system H protein	contributes_to glycine dehydrogenase (decarboxylating) activity	glycine decarboxylation via glycine cleavage system	-0.6339769363
P79023	<i>ARO4</i>	Phospho-2-dehydro-3-deoxyheptonate aldolase, tyrosine-inhibited	3-deoxy-7-phosphoheptulonate synthase activity	aromatic amino acid family biosynthetic process; chorismate biosynthetic process	0.4106874466
Carbohydrate metabolism					
A0A1D8PKW2	<i>FBP1</i>	Fructose 1,6-bisphosphate phosphatase	1- fructose 1,6-bisphosphate phosphatase activity	1- gluconeogenesis	-1.522006989
A0A1D8PLY4	<i>PYC2</i>	Pyruvate carboxylase	ATP binding; biotin binding; metal ion binding; pyruvate carboxylase activity	gluconeogenesis; pyruvate metabolic process	0.6235904694
A0A1D8PNK3	<i>GRE3</i>	Trifunctional reductase/xylose reductase/glucose 1-dehydrogenase (NADP(+))	aldehyde oxidoreductase activity	D-xylose catabolic process; arabinose catabolic process; cellular response to osmotic stress; cellular response to oxidative stress; galactose catabolic process; oxidation-reduction process	-0.9825048447
A0A1D8PS79	<i>IDP2</i>	Isocitrate dehydrogenase [NADP]	isocitrate dehydrogenase (NADP+) activity; magnesium ion binding; cycle NAD binding	isocitrate metabolic process; tricarboxylic acid cycle	-2.973912239
A0A1D8PSH3	<i>CIT1</i>	Citrate synthase	ATP citrate synthase activity; citrate (Si)-synthase activity	tricarboxylic acid cycle	-0.8699102402
A0A1D8PSZ0	<i>IFE2</i>	Ife2p	oxidoreductase activity; zinc ion binding	oxidation-reduction process	-1.208379745
A0A1D8PU04	CAALFM_C R09670CA	S-formylglutathione hydrolase	S-formylglutathione hydrolase activity	formaldehyde catabolic process	0.6277980804
A0A1D8PU61	<i>FDH3</i>	S-(hydroxymethyl)glutathione dehydrogenase	S-(hydroxymethyl)glutathione dehydrogenase activity; zinc ion binding	cell redox homeostasis; cellular response to oxidative stress; pathogenesis; glycine catabolic process; amino acid catabolic process to alcohol via Ehrlich pathway; ethanol oxidation; formaldehyde catabolic process; furaldehyde metabolic process; oxidation-reduction process	0.5219736099

P83773	<i>ACH1</i>	Acetyl-CoA hydrolase	acetyl-CoA hydrolase activity	acetate metabolic process; acetyl-CoA metabolic process; cellular response to alkaline pH	-0.7261962891
P83778	<i>MDH1</i>	Malate dehydrogenase, cytoplasmic	L-malate dehydrogenase activity; malate dehydrogenase activity	carbohydrate metabolic process; malate metabolic process; tricarboxylic acid cycle	-2.016073227
Q5A0Z9	<i>PDA1</i>	Pyruvate dehydrogenase E1 component subunit alpha	pyruvate dehydrogenase (acetyl-transferring) activity	acetyl-CoA biosynthetic process from pyruvate	0.6566324234
Q5A5V6	<i>PDB1</i>	Pyruvate dehydrogenase E1 component subunit beta	pyruvate dehydrogenase (acetyl-transferring) activity	acetyl-CoA biosynthetic process from pyruvate; glycolytic process	0.5407962799
Q5AGX8	<i>LAT1</i>	Acetyltransferase component of pyruvate dehydrogenase complex	dihydrolipoyllysine-residue acetyltransferase activity	pyruvate metabolic process	0.727148056
Q5AKV6	<i>PDX1</i>	Pdx1p	transferase activity, transferring acyl groups	filamentous growth; metabolic process; single-species biofilm formation on inanimate substrate	0.5077676773
Q5AKX2	<i>OSM2</i>	Fumarate reductase	heme binding; metal ion binding; succinate dehydrogenase activity	FAD metabolic process; oxidation-reduction process; protein folding in endoplasmic reticulum	0.7646503448
Q5AKX8	<i>CYB2</i>	Cyb2p	heme binding; L-lactate dehydrogenase (cytochrome) activity; metal ion binding	entry into host through natural portals; lactate metabolic process; metabolism by symbiont of substance in host	0.5137434006
Lipid metabolism					
A0A1D8PH78	<i>ERG20</i>	Bifunctional (2E,6E)-farnesyl diphosphate synthase/dimethylallyltransferase	dimethylallyltransferase activity; geranyltransferase activity	ergosterol biosynthetic process; isoprenoid biosynthetic process	0.9012012482
Protein biosynthesis/folding					
A0A1D8PN90	<i>STI1</i>	Hsp90 cochaperone	ATPase inhibitor activity; protein binding; Hsp90 binding; mRNA binding	Hsp70 protein folding; protein targeting to protein mitochondrion	-0.4388208389

P25997	<i>CEF3</i>	Elongation factor 3	ATPase activity; ATP binding; translational elongation GTPase activity; translation elongation factor activity			0.4013900757
Glyoxylate cycle						
Q5APD2	<i>MLS1</i>	Malate synthase	malate synthase activity		glyoxylate cycle; tricarboxylic acid cycle	-2.737627983
Stress response						
A0A1D8PLJ3	<i>SOD1</i>	Superoxide dismutase [Cu-Zn]	metal ion binding; superoxide dismutase activity	cellular response to oxidative stress; filamentous growth; filamentous growth of a population of unicellular organisms in response to starvation; pathogenesis		-2.281773567
A0A1D8PQH5	<i>SOD3</i>	Superoxide dismutase	metal ion binding; superoxide dismutase activity	age-dependent response to oxidative stress involved in chronological cell aging; oxidation-reduction process; removal of superoxide radicals		1.609313965
A0A1D8PS56	<i>ECM4</i>	Omega-class transferase	glutathione glutathione transferase activity	cellular response to starvation; filamentous growth; filamentous growth of a population of unicellular organisms in response to biotic stimulus; filamentous growth of a population of unicellular organisms in response to starvation		-0.2444143295
O13289	<i>CAT1</i>	Peroxisomal catalase	catalase activity; heme binding; metal ion binding	cellular response to hydrogen peroxide; cellular response to starvation; filamentous growth; filamentous growth of a population of unicellular organisms in response to chemical stimulus; filamentous growth of a population of unicellular organisms in response to starvation; hydrogen peroxide catabolic process; hydrogen peroxide metabolic process; interaction with host; pathogenesis; response to hydrogen peroxide		-0.3804578781
Q59MV9	<i>YHB1</i>	Flavoheomprotein	heme binding; metal ion binding; nitric oxide dioxygenase activity; oxygen binding	cellular response to nitrosative stress; filamentous growth; filamentous growth of a population of unicellular organisms; nitric		0.6299734116

				oxide catabolic process; pathogenesis; response to defense-related host nitric oxide production; response to toxic substance	
Q59WW7	<i>GPS2/orf19.86</i>	Glutathione peroxidase	glutathione peroxidase activity	response to oxidative stress	-0.959485054
Q5A5A0	<i>PRX1</i>	Thioredoxin peroxidase	thioredoxin peroxidase activity	cell redox homeostasis; cellular response to oxidative stress	-0.4752588272
Q5ABB1	<i>TTR1</i>	Dithiol glutaredoxin	electron transfer activity; protein disulfide oxidoreductase activity	cell redox homeostasis; cellular response to oxidative stress; pathogenesis	-0.4375391006
Ribosome					
A0A1D8PDL6	orf19.2478.1	Ribosomal 60S subunit protein L7A	cellular component	cytoplasmic translation (IEA with <i>S. cerevisiae</i> : RPL7A) e maturation of LSU-rRNA	0.5493927002
A0A1D8PDP4	<i>RPS27A</i>	40S ribosomal protein S27	metal ion binding e structural constituent of ribosome	translation	-0.8073043823
A0A1D8PU46	<i>SIK1</i>	snoRNP complex protein	unknown	rRNA processing	0.2416696548
Q59S06	<i>NOP58</i>	Nucleolar protein 58	unknown	filamentous growth; rRNA processing	0.3969116211
Q5A0V9	<i>NOPI</i>	rRNA methyltransferase	methyltransferase activity; RNA binding	rRNA processing	0.4075584412
Metabolism of cofactors and vitamins					
Q5A3V6	<i>RIB3</i>	3,4-dihydroxy-2-butanone 4-phosphate synthase	3,4-dihydroxy-2-butanone-4-phosphate synthase activity; metal ion binding	riboflavin biosynthetic process	0.7043361664
Q5A3Y5	<i>THI13</i>	4-amino-5-hydroxymethyl-2-methylpyrimidine phosphate synthase	thiamine pyrophosphate binding	thiamine biosynthetic process; thiamine diphosphate biosynthetic process	1.331450462
Q5ANB7	<i>THI4</i>	Thiamine thiazole synthase	metal ion binding	response to stress; thiamine biosynthetic process	1.799358368
Energy					

A0A1D8PJ01	<i>PMA1</i>	Plasma membrane ATPase	ATPase activity; ATP binding; metal ion binding; proton-exporting ATPase activity, phosphorylative mechanism	proton export across plasma membrane	0.7011356354
Q5AP79	<i>MIR1</i>	Mir1p	phosphate ion transmembrane transporter activity	phosphate ion transport	0.4497089386
Q59ZE0	<i>ATP4</i>	F1F0 ATP synthase subunit 4	proton transmembrane transporter activity	ATP synthesis coupled proton transport	0.225028038
Others					
A0A1D8PD78	<i>IFD6</i>	Ifd6p	oxidoreductase activity e aryl-alcohol dehydrogenase (NAD+) activity	single-species biofilm formation on inanimate substrate	1.287586212
A0A1D8PDA4	<i>FMA1</i>	Fma1p	oxidoreductase activity	metabolic process	0.8170814514
A0A1D8PHQ3	orf19.36.1	Uncharacterized protein	unknown	unknown	-0.6240568161
O13318	<i>PHR2</i>	pH-responsive protein 2	1,3-beta-glucanosyltransferase activity; glucanosyltransferase activity	fungal-type cell wall organization; pathogenesis	0.7462463379
Q59KV8	<i>LSP1</i>	Lipid-binding protein	lipid binding	eisosome assembly; endocytosis; negative regulation of protein kinase activity; negative regulation of sphingolipid biosynthetic process; protein localization to eisosome filament; response to heat	-0.4921894073
Q59Y31	<i>YWP1</i>	Yeast-form wall Protein 1	unknown	adhesion of symbiont to host; cell adhesion; single-species biofilm formation	0.5545415878
Q5AK88	orf19.3932	Uncharacterized protein	nucleic acid binding	unknown	-0.3563690186

*Difference of the protein intensities between P1 and wild type strain, positive value indicating increased in abundance in P1 and negative value indicating decreased in abundance in P1.

Molecular function and biological process according to UniProt and *Candida* genome database.

Table S2. Identification of proteins from *Candida albicans* (Passage 3) by mass spectrometry

Protein IDs	Gene name	UniProt names	Molecular function	Biological process	*Difference
Amino acid metabolism					
A0A1D8PGT5	<i>ALD5</i>	Aldehyde dehydrogenase (NAD(P)(+))	oxidoreductase activity, acting on the aldehyde or oxo group of donors, NAD or NADP as acceptor	acetate biosynthetic process; oxidation-reduction process	-0.7793941498
A0A1D8PMH8	<i>GDH3</i>	Glutamate dehydrogenase	oxidoreductase activity, acting on the CH-NH2 group of donors, NAD or NADP as acceptor	cellular amino acid metabolic process	-0.6970434189
Q5A362	<i>CYS3</i>	Cystathionine gamma-lyase	cystathionine gamma-lyase activity; pyridoxal phosphate binding	cysteine biosynthetic process via cystathionine; methionine biosynthetic process; transsulfuration	0.681183815
Carbohydrate metabolism					
A0A1D8PKV4	<i>FUM12</i>	Fum12p	fumarate hydratase activity	fumarate metabolic process; tricarboxylic acid cycle	-0.4057559967
A0A1D8PKW2	<i>FBP1</i>	Fructose 1,6-bisphosphate phosphatase	fructose 1,6-bisphosphate phosphatase activity	gluconeogenesis	-1.168065071
A0A1D8PSH3	<i>CIT1</i>	Citrate synthase	ATP citrate synthase activity; (Si)-synthase activity	tricarboxylic acid cycle	-1.065693855
A0A1D8PSZ0	<i>IFE2</i>	Ife2p	oxidoreductase activity; zinc ion binding	oxidation-reduction process	-1.049014091
P83773	<i>ACH1</i>	Acetyl-CoA hydrolase	acetyl-CoA hydrolase activity	acetate metabolic process; acetyl-CoA metabolic process; cellular response to alkaline pH	-0.6624755859
Q5AED0	orf19.338	Uncharacterized protein	mannosyl-oligosaccharide glucosidase activity	oligosaccharide metabolic process	-0.4185562134
Q8NJN3	<i>ACS2</i>	Acetyl-coenzyme synthetase 2	acetate-CoA ligase activity; AMP binding; ATP binding	acetyl-CoA biosynthetic process; acetyl-CoA biosynthetic process from acetate	-0.4514570236
Lipid metabolism					

A0A1D8PRR7	<i>ACC1</i>	Acetyl-CoA carboxylase	acetyl-CoA carboxylase activity; ATP binding; metal ion binding	fatty acid biosynthetic process	-0.3735637665
Nucleic acid processing					
Q59VN4	<i>HHF22/HHF1</i>	Histone H4	DNA binding; heterodimerization activity	protein DNA-templated transcription, initiation; nucleosome assembly	0.4918985367
Q5AI86	<i>TIF34</i>	Eukaryotic translation initiation factor 3 subunit I	translation initiation factor activity	cellular response to drug	0.461016655
Protein biosynthesis/folding					
A0A1D8PQ94	<i>SBA1</i>	Hsp90 cochaperone	chaperone binding	protein folding	0.7337417603
Glyoxylate cycle					
Q59RB8	<i>ICL1</i>	Isocitrate lyase	isocitrate lyase activity; metal ion binding	glyoxylate cycle; pathogenesis	-3.102285385
Q5APD2	<i>MLS1</i>	Malate synthase	malate synthase activity	glyoxylate cycle; tricarboxylic acid cycle	-3.049711227
Stress response					
A0A1D8PLJ3	<i>SOD1</i>	Superoxide dismutase [Cu-Zn]	metal ion binding; superoxide dismutase activity	cellular response to oxidative stress; filamentous growth; filamentous growth of a population of unicellular organisms in response to starvation; pathogenesis	-2.582626343
A0A1D8PQH5	<i>SOD3</i>	Superoxide dismutase	metal ion binding; superoxide dismutase activity	age-dependent response to oxidative stress involved in chronological cell aging; oxidation-reduction process; removal of superoxide radicals	1.941585541
O13289	<i>CAT1</i>	Peroxisomal catalase	catalase activity; heme binding; metal ion binding	cellular response to hydrogen peroxide; cellular response to starvation; filamentous growth; filamentous growth of a population of unicellular organisms in response to chemical stimulus; filamentous growth of a population of unicellular organisms in response to starvation; hydrogen peroxide catabolic process; hydrogen peroxide metabolic process;	-0.4710092545

Q59MV9	<i>YHB1</i>	Flavoheomoprotein	heme binding; metal ion binding; nitric oxide dioxygenase activity; oxygen binding	interaction with host; pathogenesis; response to hydrogen peroxide	0.5347242355
Metabolism of cofactors and vitamins					
Q5A3V6	<i>RIB3</i>	3,4-dihydroxy-2-butanone phosphate synthase	4- 3,4-dihydroxy-2-butanone-4-phosphate synthase activity; metal ion binding	riboflavin biosynthetic process	0.4435052872
Q5A3Y5	<i>THI13</i>	4-amino-5-hydroxymethyl-2-methylpyrimidine phosphate synthase	thiamine pyrophosphate binding	thiamine biosynthetic process; thiamine diphosphate biosynthetic process	0.8529376984
Energy metabolism					
Q9B8D8	<i>COX2</i>	Cytochrome c oxidase subunit 2	copper ion binding; cytochrome-c oxidase activity	mitochondrial electron transport, cytochrome c to oxygen	-0.6721410751
Others					
A0A1D8PHF8	<i>WHI1</i>	Wh11p	unknown	pathogenesis; phenotypic switching; response to stress; single-species biofilm formation on inanimate substrate	-0.8011341095
A0A1D8PHH2	<i>PNG2</i>	Png2p	peptide-N4-(N-acetyl-beta-glucosaminy)asparagine amidase activity	protein deglycosylation	0.8540554047
A0A1D8PM81	orf19.3782.2	MICOS complex subunit MIC10	unknown	cristae formation/ protein transport	-1.16242218
A0A1D8PRB4	orf19.1338	Uncharacterized protein	unknown	unknown	0.3890743256
A0A1D8PSE1	<i>MLC1</i>	Mlc1p	calcium ion binding	mitotic actomyosin contractile ring assembly; actin filament organization; protein localization to medial cortex; vesicle targeting	0.3875980377

Q59Y31	<i>YWP1</i>	Yeast-form wall Protein 1	unknown	adhesion of symbiont to host; cell adhesion; single-species biofilm formation	1.27693367
--------	-------------	---------------------------	---------	---	------------

*Difference of the protein intensities between P3 and wild type strain, positive value indicating increased in abundance in P3 and negative value indicating decreased in abundance in P3.

Molecular function and biological process according to UniProt and *Candida* genome database.

Table S3. Identification of proteins from *Candida albicans* (Passage 4) by mass spectrometry

Protein IDs	Gene name	UniProt names	Molecular function	Biological process	*Difference
Amino acid metabolism					
A0A1D8PDX5	<i>MMD1</i>	Isoleucine biosynthesis protein	deaminase activity	isoleucine biosynthetic process; mitochondrial translation	-0.4822034836
A0A1D8PF68	<i>SAM2</i>	S-adenosylmethionine synthase	ATP binding; metal ion binding; methionine adenosyltransferase activity	one-carbon metabolic process; S-adenosylmethionine biosynthetic process	0.6287565231
A0A1D8PGT5	<i>ALD5</i>	Aldehyde dehydrogenase (NAD(P)(+))	oxidoreductase activity, acting on the aldehyde or oxo group of donors, NAD or NADP as acceptor	acetate biosynthetic process; oxidation-reduction process	-0.6962976456
A0A1D8PIB2	<i>ASN1</i>	Asparagine synthase (Glutamine-hydrolyzing) 2	asparagine synthase (glutamine-hydrolyzing) activity; ATP binding	asparagine biosynthetic process; glutamine metabolic process	0.2279081345
A0A1D8PJR2	<i>GTT11</i>	Gtt11p	glutathione transferase activity	unknown	-0.580198288
A0A1D8PRR5	<i>ARG1</i>	argininosuccinate synthase	argininosuccinate synthase activity; ATP binding	arginine biosynthetic process	-0.7058420181
P83783	<i>SAH1</i>	Adenosylhomocysteinase	adenosylhomocysteinase activity; NAD binding	one-carbon metabolic process; S-adenosylhomocysteine catabolic process	0.4408073425
Q59MU3	<i>ARO10</i>	Phenylpyruvate decarboxylase	carboxy-lyase activity; metal ion binding; thiamine pyrophosphate binding; phenylpyruvate decarboxylase activity	aromatic amino acid family catabolic process to alcohol via Ehrlich pathway	-0.4963207245

Q59N40	<i>AAT21</i>	Aspartate aminotransferase	L-aspartate:2-oxoglutarate aminotransferase activity; pyridoxal phosphate binding	biosynthetic process; cellular amino acid metabolic process	-0.5414867401
Q59R18	<i>DED81</i>	Asparagine--tRNA ligase	asparagine-tRNA ligase activity; ATP binding; nucleic acid binding	asparaginyl-tRNA aminoacylation	0.5847959518
Q59RI1	<i>ILS1</i>	Isoleucine--tRNA ligase	aminoacyl-tRNA editing activity; ATP binding; isoleucine-tRNA ligase activity; tRNA binding	isoleucyl-tRNA aminoacylation	-0.3195981979
Q5A362	<i>CYS3</i>	Cystathionine gamma-lyase	lyase activity; pyridoxal phosphate binding	cysteine biosynthetic process via cystathionine; methionine biosynthetic process; transsulfuration	0.9481925964
Carbohydrate metabolism					
A0A1D8PKV4	<i>FUM12</i>	Fum12p	fumarate hydratase activity	fumarate metabolic process; tricarboxylic acid cycle	-0.724240303
A0A1D8PKW2	<i>FBP1</i>	Fructose 1,6-bisphosphate 1-phosphatase	fructose 1,6-bisphosphate 1-phosphatase activity	gluconeogenesis	-1.452363968
A0A1D8PLY4	<i>PYC2</i>	Pyruvate carboxylase	ATP binding; biotin binding; metal ion binding; pyruvate carboxylase activity	gluconeogenesis; pyruvate metabolic process	0.3502264023
A0A1D8PNK3	<i>GRE3</i>	Trifunctional reductase/xylose reductase/glucose 1-dehydrogenase (NADP(+))	aldehyde oxidoreductase activity	D-xylose catabolic process; arabinose catabolic process; cellular response to osmotic stress; cellular response to oxidative stress; galactose catabolic process; oxidation-reduction process	-0.9244403839
A0A1D8PP43	<i>ADH1</i>	Adh1p	alcohol dehydrogenase (NAD) activity; methylglyoxal reductase (NADH-dependent) activity; zinc ion binding	induction by symbiont of host defense response; interaction with host; single-species biofilm formation in or on host organism; single-species biofilm formation on inanimate substrate	0.8220968246
A0A1D8PS79	<i>IDP2</i>	Isocitrate [NADP] dehydrogenase	isocitrate dehydrogenase (NADP+) activity; magnesium ion binding; NAD binding	isocitrate metabolic process; tricarboxylic acid cycle	-2.27148819

A0A1D8PSA9	<i>PGM2</i>	phosphoglucomutase	intramolecular transferase activity, carbohydrate metabolic process phosphotransferases; magnesium ion binding	-0.3903055191
A0A1D8PSH3	<i>CIT1</i>	Citrate synthase	ATP citrate synthase activity; citrate tricarboxylic acid cycle (Si)-synthase activity	-1.223953247
A0A1D8PSZ0	<i>IFE2</i>	Ife2p	oxidoreductase activity; zinc ion oxidation-reduction process binding	-1.499850273
A0A1D8PUB4	<i>XYL2</i>	L-iditol 2-dehydrogenase	oxidoreductase activity; zinc ion oxidation-reduction process binding	-0.3436594009
O93827	<i>MPG1/SRBI</i>	Mannose-1-phosphate guanylyltransferase	GTP binding; mannose-1-phosphate guanylyltransferase activity	0.3982839584
P40953	<i>CHT2</i>	Chitinase 2	chitinase activity; chitin binding	-0.5086317062
P46614	<i>CDC19</i>	Pyruvate kinase	ATP binding; kinase activity; magnesium ion binding; potassium ion binding; pyruvate kinase activity	0.5644741058
P83773	<i>ACH1</i>	Acetyl-CoA hydrolase	acetyl-CoA hydrolase activity	-1.031401634
P83778	<i>MDH1</i>	Malate dehydrogenase, cytoplasmic	L-malate dehydrogenase activity; malate dehydrogenase activity	-1.569755554
P83779	<i>PDC11</i>	Pyruvate decarboxylase	magnesium ion binding; pyruvate decarboxylase activity; thiamine pyrophosphate binding	0.4423465729

Q5A850	<i>GSY1</i>	Glycogen [starch] synthase	glycogen (starch) synthase activity	glycogen biosynthetic process	-0.2303543091
Q5AGZ8	<i>PFK2</i>	ATP-dependent phosphofructokinase	6- 6-phosphofructokinase activity; ATP binding; metal ion binding	fructose 6-phosphate metabolic process; glycolytic process	0.3181686401
Q5AKX2	<i>OSM2</i>	Fumarate reductase	heme binding; metal ion binding; succinate dehydrogenase activity	FAD metabolic process; oxidation-reduction process; protein folding in endoplasmic reticulum	0.5936632156
Q5AKX8	<i>CYB2</i>	Cyb2p	heme binding; L-lactate dehydrogenase (cytochrome) activity; metal ion binding	entry into host through natural portals; lactate metabolic process; metabolism by symbiont of substance in host	0.3186035156
Q5AMP4	<i>MDH1-1</i>	Malate dehydrogenase	L-malate dehydrogenase activity	carbohydrate metabolic process; malate metabolic process; tricarboxylic acid cycle	-0.5831956863
Q8NJJ3	<i>ACS2</i>	Acetyl-coenzyme A synthetase 2	acetate-CoA ligase activity; AMP binding; ATP binding	acetyl-CoA biosynthetic process; acetyl-CoA biosynthetic process from acetate	-0.4534273148
Lipid metabolism					
A0A1D8PQN3	<i>ACB1</i>	Long-chain fatty acid transporter	long-chain fatty acyl-CoA binding	chronological cell aging; very long-chain fatty acid biosynthetic process	1.179416656
A0A1D8PQP7	<i>CYB5</i>	Cyb5p	electron transfer activity; heme binding; metal ion binding	ergosterol biosynthetic process	0.4321460724
A0A1D8PH52	<i>ERG10</i>	Acetyl-CoA acetyltransferase	C- transferase activity, transferring acyl groups other than amino-acyl groups	metabolic process	-0.5487518311
A0A1D8PRR7	<i>ACC1</i>	Acetyl-CoA carboxylase	acetyl-CoA carboxylase activity; ATP binding; metal ion binding	fatty acid biosynthetic process	-0.4630470276
Q5A7M9	<i>RHR2</i>	Glycerol-1-phosphatase	glycerol-3-phosphatase activity; phosphatase activity	cell-abiotic substrate adhesion; cellular response to osmotic stress; entry into host; glycerol biosynthetic process; glycerol metabolic process; pathogenesis; single-species biofilm formation on inanimate substrate	0.721950531
Nucleic acid processing					
A0A1D8PFX4	orf19.7256	RNA-binding protein	contributes_to RNA binding; poly(U) RNA binding	mRNA splicing, via spliceosome	1.159379005

A0A1D8PH31	<i>TAF14</i>	TATA-binding associated factor	protein-DNA-binding transcription factor activity; contributes_to DNA translocase activity; TBP-class protein binding; transcription factor activity, core RNA polymerase II binding	positive regulation of cell adhesion involved in single-species biofilm formation; positive regulation of cell-substrate adhesion; regulation of single-species biofilm formation on inanimate substrate; regulation of transcription by RNA polymerase II; single-species biofilm formation on inanimate substrate	-0.2888507843
Q59WG0	<i>HNT1</i>	Adenosine monophosphoramidase	5'-catalytic activity	nucleotide metabolic process	-1.065743446
Q5AG96	orf19.4283	Uncharacterized protein	translation initiation factor activity	cytoplasmic translational initiation	-0.5718517303
Q9P975	<i>TIF45</i>	Eukaryotic translation initiation factor 4E	translation initiation factor activity	regulation of translation; translational initiation	-0.6807031631
Protein biosynthesis/folding					
A0A1D8PFU8	orf19.7215.3	Uncharacterized protein	chaperone binding; unfolded protein binding	protein folding; chaperone-mediated protein complex assembly; protein import into mitochondrial intermembrane space	-0.8519191742
A0A1D8PJ20	<i>SCL1</i>	Proteasome complex	endopeptidase threonine-type endopeptidase activity	ubiquitin-dependent protein catabolic process	-0.8875684738
A0A1D8PM35	<i>EFB1</i>	Translation elongation factor 1 subunit beta	translation elongation factor activity	translational elongation	-0.3518152237
A0A1D8PRB6	<i>PUP3</i>	proteasome core particle subunit beta 3	threonine-type endopeptidase activity	proteasome-mediated ubiquitin-dependent protein catabolic process	-0.4264621735
A0A1D8PRC2	<i>CPY1</i>	carboxypeptidase	serine-type carboxypeptidase activity	macroautophagy; phytochelatin biosynthetic process; zymogen activation	0.6612825394
O94083	<i>ANB1</i>	Eukaryotic translation initiation factor 5A	ribosome binding; translation elongation factor activity	positive regulation of translational elongation; positive regulation of translational termination; translational frameshifting	-0.4636182785
Q5A0L8	<i>PR26</i>	Proteasome regulatory particle base subunit	ATP binding; proteasome-activating ATPase activity; hydrolase activity; nucleoside-triphosphatase activity; nucleotide binding	protein catabolic process	-0.4392995834

Q5ALM6	<i>CPR3</i>	Peptidyl-prolyl isomerase	cis-trans	peptidyl-prolyl activity	cis-trans isomerase	protein folding; apoptotic process; protein peptidyl-prolyl isomerization	-0.6788568497
Q59WE2	<i>SKP1</i>	SCF ubiquitin ligase subunit		ligase activity		ubiquitin-dependent protein catabolic process	0.5514116287
Glyoxylate cycle							
Q59RB8	<i>ICL1</i>	Isocitrate lyase		isocitrate lyase activity; metal ion binding		glyoxylate cycle; pathogenesis	-4.157952309
Q5APD2	<i>MLS1</i>	Malate synthase		malate synthase activity		glyoxylate cycle; tricarboxylic acid cycle	-3.086671829
Stress response							
A0A1D8PLJ3	<i>SOD1</i>	Superoxide dismutase [Cu-Zn]		metal ion binding; dismutase activity	superoxide	cellular response to oxidative stress; filamentous growth; filamentous growth of a population of unicellular organisms in response to starvation; pathogenesis	-1.731225967
A0A1D8PMP0	<i>OYE32</i>	Oye32p		FMN binding; oxidoreductase activity		cell redox homeostasis	0.6551866531
A0A1D8PQH5	<i>SOD3</i>	Superoxide dismutase		metal ion binding; dismutase activity	superoxide	age-dependent response to oxidative stress involved in chronological cell aging; oxidation-reduction process; removal of superoxide radicals	2.057108879
A0A1D8PS56	<i>ECM4</i>	Omega-class transferase	glutathione	glutathione transferase activity		cellular response to starvation; filamentous growth; filamentous growth of a population of unicellular organisms in response to biotic stimulus; filamentous growth of a population of unicellular organisms in response to starvation	-0.4098491669
A0A1D8PSE7	<i>IFR2</i>	Ifr2p		oxidoreductase activity		oxidation-reduction process	-0.5328969955
A0A1D8PTP9	<i>HSP104</i>	chaperone ATPase		ATPase activity, coupled; binding	ATP	cellular heat acclimation; cellular response to heat; chaperone cofactor-dependent protein refolding; pathogenesis; protein metabolic process; single-species biofilm formation on inanimate substrate	-0.2231674194
O13289	<i>CAT1</i>	Peroxisomal catalase		catalase activity; heme binding; metal ion binding		cellular response to hydrogen peroxide; cellular response to starvation; filamentous	-0.3214054108

				growth; filamentous growth of a population of unicellular organisms in response to chemical stimulus; filamentous growth of a population of unicellular organisms in response to starvation; hydrogen peroxide catabolic process; hydrogen peroxide metabolic process; interaction with host; pathogenesis; response to hydrogen peroxide	
O74261	<i>HSP60</i>	Heat shock protein 60, mitochondrial	ATP binding	cellular response to heat; protein refolding	-0.2773160934
P0CT51	<i>BLP1</i>	Blood-induced peptide 1	unknown	unknown	1.216862679
Q59MV9	<i>YHB1</i>	Flavohepotein	heme binding; metal ion binding; nitric oxide dioxygenase activity; oxygen binding	cellular response to nitrosative stress; filamentous growth; filamentous growth of a population of unicellular organisms; nitric oxide catabolic process; pathogenesis; response to defense-related host nitric oxide production; response to toxic substance	0.3077068329
Q59X49	<i>DDR48</i>	Stress protein DDR48	ATPase activity; GTPase activity	cellular response to oxidative stress; cellular response to starvation; DNA repair; filamentous growth; filamentous growth of a population of unicellular organisms in response to biotic stimulus and to starvation	1.294729233
Q5A7P9	<i>DOT5</i>	Thioredoxin peroxidase	peroxidase activity	cell redox homeostasis	-0.483587265
Q5AEN1	<i>CCP1</i>	Cytochrome c peroxidase, mitochondrial	cytochrome-c peroxidase activity; heme binding; metal ion binding	cellular response to oxidative stress; cellular response to reactive oxygen species	0.3090362549
Mitochondrial biogenesis					
A0A1D8PM81	orf19.3782.2	MICOS complex subunit MIC10	unknown	cristae formation	-1.53439045
Q59R24	<i>TIM9</i>	Mitochondrial import inner membrane translocase subunit TIM9	metal ion binding	protein transport	0.7146520615
Q5AH14	<i>TOM40</i>	Tom40p	protein transmembrane transporter activity	protein import into mitochondrial matrix	-0.4477071762

Q5AND0	<i>PHB2</i>	Prohibitin subunit	unknown	mitochondrion inheritance; negative regulation of proteolysis; protein folding; replicative cell aging	-0.3015499115
Ribosome					
A0A1D8PTS0	<i>RPP2A</i>	ribosomal protein P2A	structural constituent of ribosome	translation; translational elongation	0.7037200928
A0A1D8PU46	<i>SIK1</i>	snoRNP complex protein	unknown	rRNA processing	-0.2836961746
Q5A109;Q5AD S0	<i>UBI3;UBI4</i>	Ubiquitin-ribosomal subunit protein S31 fusion protein/ Ubiquitin	40S protein tag; structural constituent of ribosome/ protein tag	protein ubiquitination; ribosome biogenesis; translation/ cell morphogenesis; cellular response to heat; filamentous growth; filamentous growth of a population of unicellular organisms; pathogenesis; phenotypic switching; protein ubiquitination	0.6953516006
Q5AGZ7	<i>RPL5</i>	Ribosomal 60S subunit protein L5	5S rRNA binding; structural constituent of ribosome	translation	-0.4783248901
Metabolism of cofactors and vitamins					
A0A1D8PHR5	<i>PST1</i>	Pst1p	FMN binding; NAD(P)H dehydrogenase (quinone) activity; oxidoreductase activity, acting on NAD(P)H, quinone or similar compound as acceptor	cellular response to oxidative stress; pathogenesis ; negative regulation of transcription, DNA-templated	-1.439580917
Q5A3V6	<i>RIB3</i>	3,4-dihydroxy-2-butanone phosphate synthase	4-3,4-dihydroxy-2-butanone-4-phosphate synthase activity; metal ion binding	riboflavin biosynthetic process	0.6501731873
Q5A3Y5	<i>THI13</i>	4-amino-5-hydroxymethyl-2-methylpyrimidine phosphate synthase	thiamine pyrophosphate binding	thiamine biosynthetic process; thiamine diphosphate biosynthetic process;	0.9725437164
Q5ANB7	<i>THI4</i>	Thiamine thiazole synthase	metal ion binding	response to stress; thiamine biosynthetic process	0.7297010422

Q59Y37	<i>PST2</i>	Pst2p	2-hydroxy-1,4-benzoquinone reductase activity; FMN binding; NAD(P)H dehydrogenase (quinone) activity	cellular response to oxidative stress; pathogenesis; negative regulation of transcription, DNA-templated	-0.5678453445
Energy & respiration					
A0A1D8PDP8	orf19.2439.1	Ubiquinol--cytochrome-c reductase subunit 10	contributes_to ubiquinol-cytochrome-c reductase activity	aerobic respiration; mitochondrial electron transport, ubiquinol to cytochrome c	-0.8264064789
A0A1D8PQD5	orf19.1082.1	cytochrome c oxidase subunit	cytochrome-c oxidase activity	mitochondrial intermembrane space; mitochondrial respiratory chain complex IV	0.5557098389
Q59KG2	<i>RGII/UCF1</i>	Respiratory growth induced protein 1	unknown	energy reserve metabolic process	-0.7740736008
Others					
A0A1D8PHH2	<i>PNG2</i>	Png2p	peptide-N4-(N-acetyl-beta-glucosaminyl)asparagine amidase activity	protein deglycosylation	2.096619606
A0A1D8PHQ3	orf19.36.1	Uncharacterized protein	unknown	unknown	1.899688721
A0A1D8PHU6	orf19.2269	Putative phosphoric monoester hydrolase	phosphatase activity	metabolic process	-0.6465187073
A0A1D8PLD7	orf19.4609	Uncharacterized protein	hydrolase activity	unknown	-0.4570531845
A0A1D8PMF8	<i>CMD1</i>	Calmodulin	calcium-dependent protein binding; calcium ion binding	cellular response to drug; filamentous growth of a population of unicellular organisms; intracellular signal transduction; phospholipid metabolic process	0.5214548111
A0A1D8PQE6	orf19.2125	Uncharacterized protein	unknown	unknown	0.9611930847
A0A1D8PTR7	<i>TPM2</i>	Tropomyosin	actin lateral binding	actin cortical patch localization; actin cortical patch organization; actin filament bundle assembly; actin filament reorganization; mitotic actomyosin contractile ring assembly; mitotic actomyosin contractile ring contraction; ...; pseudohyphal growth	0.7659692764
G1UAZ9	orf19.5158	Uncharacterized protein	oxidoreductase activity	oxidation-reduction process	-0.59416008

O13318	<i>PHR2</i>	pH-responsive protein 2	1,3-beta-glucanosyltransferase activity; glucanosyltransferase activity	fungal-type cell wall organization; pathogenesis	1.279542923
Q59Y31	<i>YWP1</i>	Yeast-form wall Protein 1	unknown	adhesion of symbiont to host; cell adhesion; single-species biofilm formation	1.614230156
Q5A1M1	<i>TFS1</i>	Tfs1p	peptidase inhibitor activity; phospholipid binding	regulation of Ras protein signal transduction; regulation of proteolysis	-0.6290254593
Q5AD47;A0A1D8PG82	<i>HGT6;HGT8</i>	Hexose transporter/Hgt8p	transmembrane transporter activity	carbohydrate transport; transmembrane transport	0.5088605881
Q5AF37	orf19.2769	Uncharacterized protein	Unknown	Unknown	1.010421753

*Difference of the protein intensities between P4 and wild type strain, positive value indicating increased in abundance in P4 and negative value indicating decreased in abundance in P4.

Molecular function and biological process according to UniProt and *Candida* genome database.

CHAPTER II

Manuscript II: “Insights into *Candida albicans* virulence factors after serial systemic candidiasis”

Insights into *Candida albicans* virulence factors after serial systemic candidiasis

Glaucia S Arita¹, Daniella R Faria¹, Karina M Sakita¹, Franciele A V Rodrigues-Vendramini¹, Isis R G Capoci¹, Érika S Kioshima¹, Patrícia S Bonfim-Mendonça¹, Terezinha I E Svidzinski^{1*}.

¹Department of Clinical Analysis and Biomedicine, State University of Maringá, Paraná, Brazil.

*Corresponding author: Terezinha Inez Estivalet Svidzinski.

Av. Colombo, 5790

ZIP CODE: 87020-900

Maringá, PR, Brazil

Phone: +55 44 3011-4809

Fax: +55 44 3011-4860

E-mail: terezinha.svidzinski@gmail.com

Abstract

Aim: To evaluate changes in virulence and pathogenicity approaches from *Candida albicans* after successive passages in a murine model of systemic candidiasis. **Materials & methods:** Phenotypic assays were performed using colonies recovered from animals infected serially, totalizing five passages. **Results:** A progressive infection was observed along the passages, with increased fungal burden and presence of greater inflammatory areas in the histopathological findings. Furthermore, recovered strains exhibited increased filamentation and biofilm abilities, and also, a modulation of phospholipase and proteinase activities. **Conclusion:** The repeated contact between yeast and host increased expression of virulence factors that were supported by our previous proteomic data suggesting these proteins should be investigate as possible virulence markers and consequently, be targets for new antifungal agents.

Keywords: *Candida albicans* • systemic candidiasis • serial passage • virulence • morphogenesis • biofilm • phospholipase • proteinase • host–pathogen interaction

Introduction

Candida spp. are one of the most prevalent agent of nosocomial bloodstream infection, leading to higher mortality rates worldwide. Although *non-Candida albicans* (NCA) species are increasing, *C. albicans* is the most isolated yeast in episodes of candidemia [1]. This species inhabits commensally the gastrointestinal tract, vaginal mucosa, oral cavity and skin. However, an imbalance of the immune system contributes to the appearance of disease, ranging from superficial to potentially fatal disseminated candidiasis [2, 3].

The pathogenicity of *C. albicans* is related to its ability to invade host tissue and cause infection. These attributes are known as virulence factors, which can be changed during interaction with host contributing to the disease development. These factors include adherence, morphogenesis (yeast to hyphae transition) and secretion of hydrolytic enzymes [2, 4]. Recently, we showed important virulence-related proteins of *C. albicans* are expressed during the process of serial disseminated candidiasis (unpublished observations). Probably those alterations would be related with increased virulence from this microorganism and deserve to be better investigated.

Adherence on biotic or abiotic surfaces depends on cell surface adhesins expression such as agglutinin-like sequence family (Als), which is composed by eight proteins (Als1 to Als7 and Als9), with emphasis in Als3 that was present in germ tube and hyphae and when it was blocked by antibodies, *C. albicans* was not capable of adhering to cells [5, 6]. Thus, once *C. albicans* are adhered in the host cells, this pathogen has capacity to transit from yeast to hyphae form, which has been a crucial step for infection as strain unable to filament were avirulent in animals model of systemic candidiasis [7, 8]. Furthermore, secretion of hydrolytic enzymes such as phospholipase B and aspartyl proteinases (Sap) are important for pathogenesis [9]. Saps are encoded by 10 genes (*SAP1-SAP10*) and their roles are attributed in nutrients acquisition for the cells, in invasion tissue and in escape from immune system [9, 10]. When *C. albicans* strains deficient in phospholipase production were inoculated in mice through lateral tail vein, survival rates were greater than the parental strain and fungal burden were lower. They also demonstrated secretion of enzyme during invasion in the tissue, confirming virulence association with phospholipase activity [11, 12]. Furthermore, production of phospholipase and proteinase were detected in strains isolated from patients with candidemia [13, 14].

Biofilm formation is another important virulence attribute in the *C. albicans* pathogenesis. Many studies related the use of central venous catheter (CVC) as one of the main risk factors for bloodstream infection [13-15]. In addition, *C. albicans* has great ability to

produce biofilm in abiotic and biotic surfaces [16-18]. Moreover, biofilm is related to persistent candidemia [19, 20] and high resistance to antifungal therapy [21, 22].

The serial contact with the host appears to be key factor to modify the virulence factors of *C. albicans* [23, 24]. In addition, our previous findings demonstrated that virulence-related proteins of *C. albicans* were differentially expressed during the process of serial disseminated candidiasis (unpublished observations). Thus, from the insights of our previous work, the objective of this study is to phenotypically evaluate virulence factors related to *C. albicans* pathogenesis comparing with our proteomic evidence, to understand if the proteins found can be referenced as virulence markers.

Materials & methods

Strain & culture conditions

C. albicans wild-type strain SC5314 (WT) stored at Medical Mycology Laboratory at State University of Maringá, was used for the first round of infection in a murine model of disseminated candidiasis. Before each experiment, it was cultured in Sabouraud Dextrose Broth (SDB; Difco™, Detroit, MI, USA). Next, a loop was streaked on CHROMagar™ *Candida* (Becton Dickinson, Sparks, MD, USA). Then, a single colony was streaked on Sabouraud Dextrose Agar (SDA; Difco™, Detroit, MI, USA) plate and incubated for 24 h at 35°C. An inoculum of 3.5×10^6 cells/ml was prepared in Phosphate Buffered Saline (PBS; pH 7.4).

Murine model of serial disseminated candidiasis

A murine model of experimental *C. albicans* disseminated infection was used for serial infection protocol, which consists of five serial passages (P1-P5) in animals. The experiment were performed in duplicate. Mice were infected with 0.1 ml of prepared inoculum from WT strain. Then, five days post-infection, colonies recovered from kidneys of these animals, after disseminated candidiasis (P1), were used to prepare a new inoculum to infect more animals in successive passages (P2-P5). Four female Balb/c mice (7-8-week old, 23-26 g) per passage were inoculated via lateral tail vein. The animals were monitored and weighted daily for five consecutive days and then, they were anesthetized by inhalation of isoflurane for blood collection by cardiac puncture and, followed by euthanasia with ketamine-xylazine administered intraperitoneally. The kidneys, spleen, liver and brain were aseptically removed. Each organ was weighed and homogenized in lysis buffer (200 mM NaCl, 5 mM EDTA, 10

mM Tris, 10% glycerol v/v, pH 8.30). One kidney was sent to histopathological analysis and the other was used for culture and colony count. The homogenate obtained from each organ was serially diluted 1:10 and 1:100, and 20 μ L were plated on SDA and incubated for 24 h at 35°C for fungal burden determination. Results were expressed as the mean of the logarithm of the number of colony-forming units per gram of organ (log CFU/g organ) for each organ and for four animals. All procedures involving animals were approved by the Ethics Committee for Animal Use (CEUA) of the State University of Maringá, Paraná, Brazil that is in accordance with the Brazil's National Council for the Control of Animal Experimentation (CONCEA).

Histopathological examinations of the kidney

One kidney from each animal was fixed in paraformaldehyde (4%). Then, placed into ethanol and embedded in paraffin. The tissue was sectioned longitudinally and stained with hematoxylin and eosin (H&E) for visualization of inflammatory cell infiltration and Gomori methenamine silver (GMS) for fungal detection. The tissues were observed by light microscope (Motic BA310, Hong Kong, China) coupled with digital camera (Motic 5, Hong Kong, China) and images captured at $\times 400$ and $\times 600$ magnification by Motic Images Plus 2.0 software.

Quantification of cytokines from tissue homogenates

The tissue homogenate for quantification of cytokines was obtained as Lüttich, Brunke, Hube, and Jacobsen with modifications [24]. Briefly, tissue homogenates from kidney, spleen, liver and brain were centrifuged at 14,000 rpm, 4°C for 15 min. Then, the supernatants were centrifuged twice, and stored at -80°C. Mouse Th1/Th2/Th17 Cytokine Kit (BD™ Cytometric Bead Array, San Jose, CA, USA) was performed according to the manufacturer's instructions.

Chlamyospore Formation

For *in vitro* chlamyospore quantification, one microliter of the infection inoculum (3.5×10^6 yeasts/ml) were streaked on corn meal (CM)-Tween 80 agar and incubated at 25°C for 7 days in the dark. The chlamyospores were quantified by counting 50 fields divided in three regions of the cover slip using $\times 200$ magnification of an optical microscope (Motic, Hong Kong, China).

Filamentation assay

The filamentation assay was performed as previously described [17]. Briefly, *Candida* cells recovered from kidney grown in SDA plate were adjusted to an inoculum of 1×10^6 yeasts/mL in Roswell Park Memorial Institute 1640 medium (RPMI; Gibco, Grand Island, NY, USA) containing L-glutamine, sodium bicarbonate, 3-(N-morpholino) propanesulfonic acid (Sigma, St. Louis, MO, USA) (pH 7.0) as buffer, and 2% glucose, with 10% fetal bovine serum (FBS). They were incubated for 4 h at 37°C. Then, the tube was centrifuged at 10,000 rpm for 5 minutes, and pellet was resuspended in 50 μ L of water. More than 100 cells (blastopore and filamentous form) were counted in duplicate in an optic microscope coupled with camera Moticam 5.0 MP (Motic BA310, Hong Kong, China) at $\times 400$ magnification. In addition, the cells were stained with calcofluor white (Sigma-Aldrich, St. Louis, MO, USA) and visualized with epifluorescence microscope (EVOS FL Cell Imaging System, Life Technologies, CA, USA) at $\times 200$ magnification.

Phospholipase assay

Phospholipase activity was assessed as previously described with modifications [25]. The medium contained SDA supplemented by 1 M NaCl, 0.005 M CaCl_2 and 8% egg yolk. Then, a loopful of the colonies recovered from kidneys grown in SDA plate was inoculated onto the prepared plates and incubated for 7 days at 37°C. Phospholipase activity was evaluated by the difference between the diameter of the colony plus zone of precipitation and the diameter of the colony only, in millimeters. Then, results were obtained by the average of duplicates. The assay was performed in duplicate and in two separate assays.

Proteinase assay

Proteinase activity was evaluated as described previously with modifications [26]. Briefly, a medium containing 1.17% (wt/vol) yeast carbon base (Difco™, Detroit, MI, USA), 0.01% yeast extract (Himedia, Mumbai, India) and 0.2% bovine serum albumin (Sigma-Aldrich, St. Louis, MO, USA) was sterilized by filtration and added to 1.6% agar previously autoclaved. Proteinase activity was measured as mentioned above for phospholipase. The assay was performed in duplicate in two different experiments.

Biofilm Characterization

CFU determination in biofilm

Firstly, biofilm formation was evaluated through CFU count as previously described with some modifications [17]. Thus, an inoculum of 1×10^5 yeasts/ml was prepared in RPMI medium, then it was added into 96-well polystyrene plate, and incubated at 37°C on a shaker at 120 rpm/min for 2 h. Then, the wells were washed with PBS to remove non-adherent cells, and 200 μ L of RPMI medium were added. The plate was incubated for a further 24 h to allow biofilm formation. After that, the medium was removed and wells were washed with sterile PBS. Then, biofilms were scraped with 300 μ L of PBS, and suspensions were vortexed for 2 min to separate cells from the matrix [27]. Next, serial dilutions were prepared in PBS and 20 μ L of each dilution were plated onto SDA and incubated for 24 h at 37°C. The number of colonies was counted and the results were given as log CFU. These experiments were performed three times and in triplicate.

Biofilm biomass quantification

Total of biomass was quantified by crystal violet (CV) staining as described previously [28]. After 24 h of incubation, wells were washed with PBS and fixed with 200 μ L of methanol for 15 min. Then, methanol was removed and plates were dried at room temperature. Next, wells were stained with 200 μ L of CV (0.1% v/v) for 5 min. Then, they were washed with sterile water and added 200 μ L of acetic acid (33% v/v) to resuspend and dissolve the biofilm. After that, the absorbance of the solution was read at 550 nm. The results were presented as Abs/cm².

Biofilm matrix extraction and quantification

Biofilm matrix was extracted and quantified in relation to protein and carbohydrate content as described previously with modifications [28]. Thus, biofilm formation was performed in a 6-well polystyrene microtiter plate in which 3 ml of inoculum of 1×10^5 yeast cells were added per well and incubated on a shaker at 37°C for 24 h. Then, each well was scraped twice with 700 μ L of PBS, totalizing 4.2 ml of suspension per sample. One millimeter of the suspension was filtered through 0.2 μ M nitrocellulose filter to determine dry weight of biofilm. The remaining solution was sonicated for 30 s at 30 W, vortexed for 2 min and centrifuged at 3000 g for 10 min. The supernatant was filtered in 0.2 μ M nitrocellulose filter and stored at -80°C for protein and carbohydrate quantification. The protein quantification was performed using Pierce® BCA Protein Assay Kit – Reducing Agent Compatible (Thermo Scientific, Rockford, IL, USA). The carbohydrate quantification was measured as described previously [29], in which phenol and sulfuric acid was used for colorimetric quantification and glucose was used as standard.

Statistical analysis

For statistical analysis, one-way analysis of variance (ANOVA) with Bonferroni's post test was performed in the assays performed. The data were analyzed by GraphPad Prism version 6.00 (GraphPad Software, San Diego, CA, USA), with values of $p < 0.05$ considered statistically significant.

Results

Fungal burden after serial systemic candidiasis

Mice were inoculated with 3.5×10^6 yeasts cells/ml via lateral tail vein and five days post-infection or when they were moribund, they were euthanized for fungal burden determination (Figure 1). Therefore, *Candida* cells recovered from kidney, brain, spleen and liver were plated onto SDA and determined as log CFU/g organ. Until P3, none significant difference in the fungal burden of all organs analyzed was detected. Firstly, kidney burden ranged from 2.988 to 5.226 log CFU/g tissue over the passages, presenting the highest value in the fourth passage with significant statistical difference between the first passage with P4 ($p = 0.0003$) and P5 ($p = 0.0030$). Furthermore, there was a significant difference between P3 and P4 ($p = 0.0009$) and P5 ($p = 0.0225$). Secondly, fungal burden in brain ranged from 0.642 to 3.727 log CFU/g organ, showing significant differences in the last two passages in comparison to the first passage ($p = 0.0011$ and $p < 0.0001$, respectively). They also presented differences between P3 and P4 ($p = 0.0158$) and P5 ($p = 0.0003$). Thirdly, tissue burden in spleen varied from 0.295 to 1.318 without significant statistical difference over the passages ($p > 0.05$). Finally, liver burden varied from 0.118 to 3.358 log CFU/g, presenting significant differences over P4 ($p = 0.0024$) and P5 ($p < 0.0001$) when compared to P1. They also exhibited differences between P3 and P4 ($p = 0.0004$) and P5 ($p = 0.0001$). Moreover, a significant increase in liver burden in P5 compared to P4 was obtained ($p = 0.0001$). Overall, a consistent progressive systemic infection can be observed after an intravenous challenge.

Histopathological examinations of the kidney

As the main target organ for systemic candidiasis [30], we removed one kidney and sent for histopathology studies which provided valuable information about presence and morphology of fungi in the tissues. By this way, we verified that the serially contact with the host increased the ability of the fungus to remain in the animal. The histopathology of the

kidney stained with GMS showed the presence of the fungus in all passages (Figure 2 A-E). Blastoconidia was detected in P1, while hyphae was not observed in this passage. In contrast, from P2 to P5, both blastoconidia and hyphae were observed; furthermore, they were not only in the cortex, but also in renal tubules and medulla. In relation to the tissue sections stained with H&E (figure F-J), a progressive reaction was observed over the passages with fewer area of inflammation detected in P1. In P2, evident tissue disorganization and edema formation were observed. P3 showed great inflammatory infiltrate areas with tissue disorganization. In P4 and P5, it is possible to observe edema and extensive inflammatory areas.

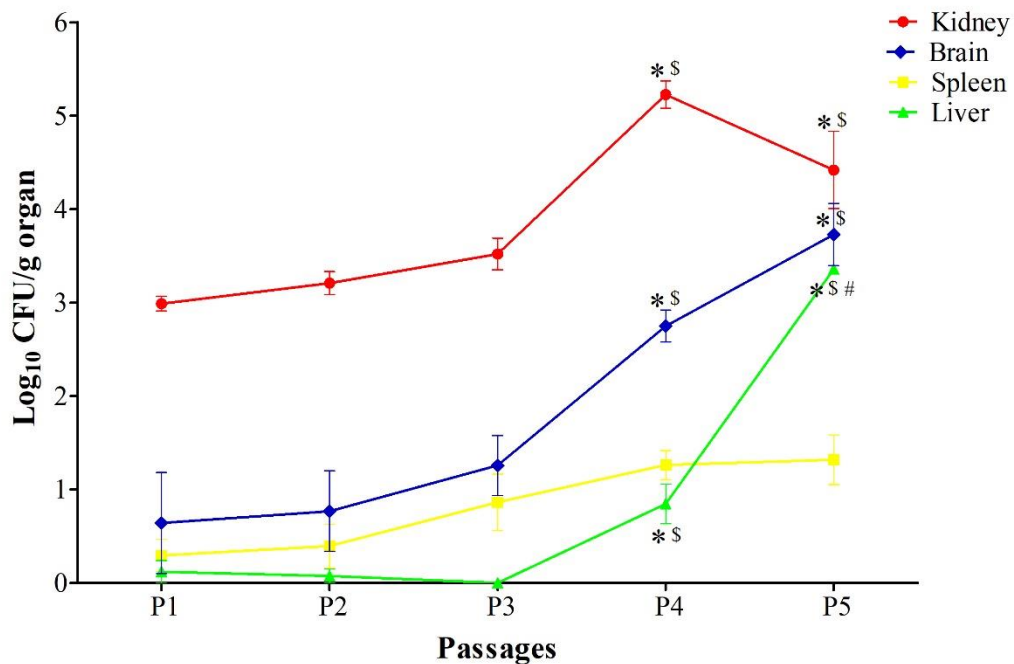


Figure 1. Model of serial systemic candidiasis increases fungal burden over the passages. Fungal burden from kidney (red), brain (blue), spleen (yellow) and liver (green) after five rounds of infection in mice (P1-P5). The results represent the average of four mice per passage. * $p < 0.05$ for fungal burden statistically different in relation to P1, \$ $p < 0.05$ to P3 and # $p < 0.05$ to P4.

Cytokines released during systemic and local immune response

As immune response play an important role during defense against *C. albicans*, we analyzed Th1, Th2 and Th17 responses from serum and kidney homogenates using the BD CBA kit in order to evaluate host immunity (Figure 3). We could detect an increase of Tumor Necrosis Factor (TNF) and Interleukin 6 (IL-6) at both, system and local immune, characteristic of an acute response to the infectious process. The other cytokines evaluated, such as Interleukin-2 (IL-2), Interleukin-4 (IL-4), Interferon- γ (IFN- γ), Interleukin-17A (IL-17A), and Interleukin-10 (IL-10) remained in the basal level below the limits of detection.

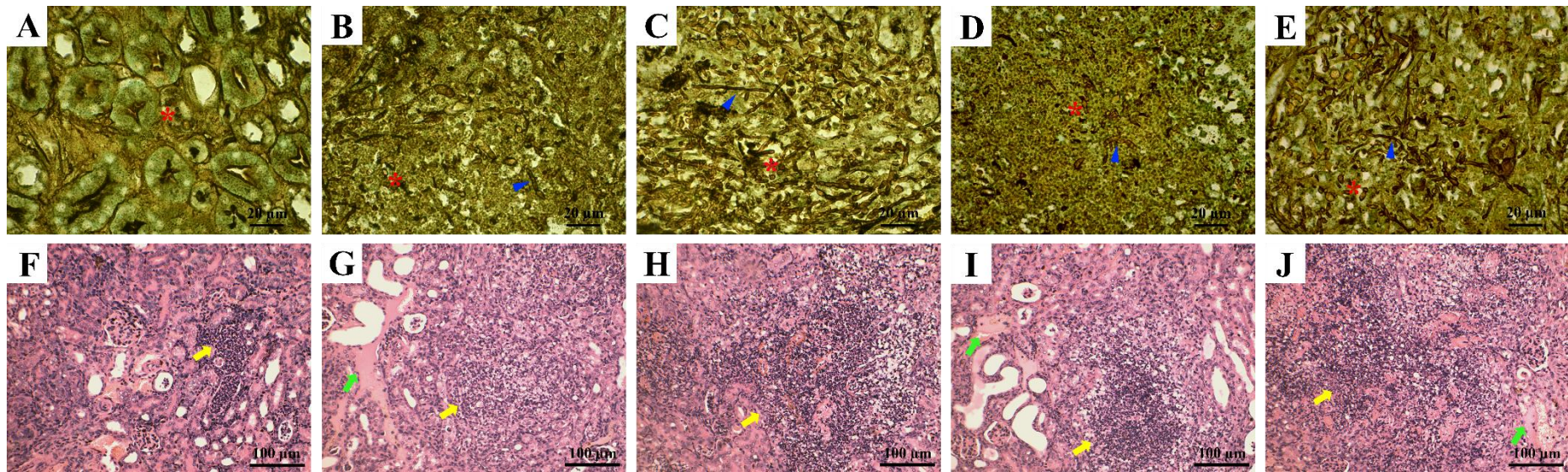


Figure 2. Histopathological alterations in the kidneys after serial systemic candidiasis in a murine model. (A-E) Tissues stained with Gomori Methenamine Silver (GMS), $\times 600$ magnification. (F-J) Tissues stained with Hematoxylin and Eosin (H&E), $\times 400$ magnification. (A & F) Tissue from passage 1 with presence of blastoconidia and inflammatory cells. (B & G) Tissue section from passage 2 containing blastoconidia and hyphae forms and inflammatory area. (C & H) Tissue section from passage 3 presenting both blastoconidia and many hyphae and an inflammatory infiltrate. (D & I) Tissue section from passage 4 demonstrating blastoconidia and hyphae forms, and inflammatory area. (E & J) Tissue section from passage 5 exhibiting blastoconidia and hyphae forms, with an extensive area of inflammatory infiltrate. Red asterisks: blastoconidia form. Blue arrowheads: hyphae form. Yellow arrows: inflammatory cells. Green arrows: edema.

Systemic immune was evidenced as a late response to *Candida* infection (Figure 3A). Until P3, a stable production of both TNF and IL-6 was detected with values from 4.96 pg/ml to 3.80 pg/ml for TNF and from 148.21 pg/ml to 217.91 pg/ml for IL-6. In contrast, there was an overexpression of TNF (87.85 pg/ml) and IL-6 (2058.67 pg/ml) in P4 that decreased for P5 in both cytokines, but maintained higher values than the other passages.

Regarding the local immune response, we choose the kidney because it is the main target organ in systemic candidiasis and showed important fungal burden as observed in Figure 1. The data show that the local response was more sensitive than the systemic, with larger and stable values since first passage. Thus, we observed an evident overproduction of IL-6 in all passages ranging from 1567.35 pg/ml in P1 to 1572.10 in P5 with highest value in P4, 3105.32 pg/ml. In the same way, there was a stable production but higher TNF over the passages with values ranging from 60.82 pg/ml in P1 to 38.58 pg/ml to P5.

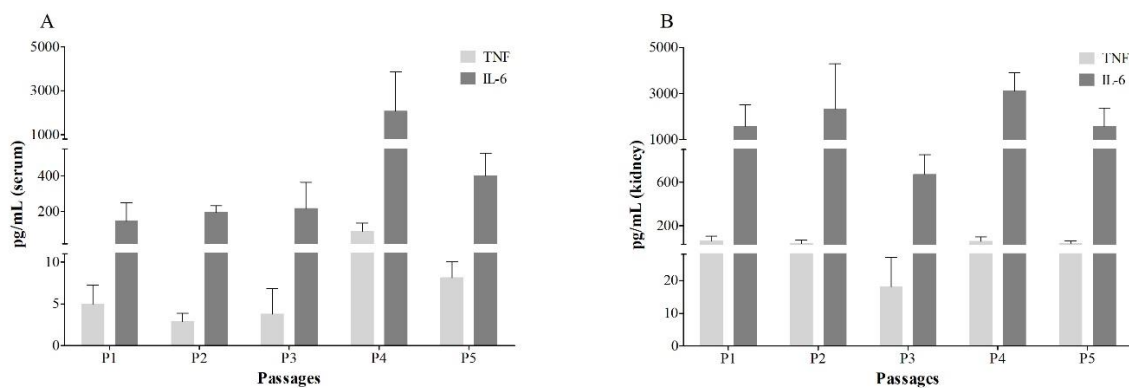


Figure 3. Cytokine production in renal tissue after serial systemic candidiasis. Evaluation of Tumor Necrosis Factor (TNF) and Interleukin-6 (IL-6) in serum (A) and in kidney (B). Animals were infected by 3.5×10^6 yeasts cells/ml. Then, their blood were collected and kidneys were removed and macerated with lysis buffer. Then, the homogenates were centrifuged to collect supernatants and stored at -80°C . Cytokine levels were analyzed by Mouse Th1/Th2/Th17 Cytokine kit. The test was performed in duplicate and statistical analysis was performed by Bonferroni's multiple comparison test.

***In vitro* quantification of chlamydospore**

During histopathological analysis, a chlamydospore-like structure was observed in the renal tissue from P3 (Figure 4A). Knowing that chlamydospore can be a predictive factor for virulence [31], we performed an *in vitro* quantification assay of chlamydospore produced in corn meal agar using yeasts recovered from P1 to P5, as represented in Figure 4B & C. The results showed an increased trend in chlamydospore formation through passages, highlighting

P3. While WT produced 59 chlamydospores, P1, P2, P3, P4 and P5 produced 138, 194, 388, 161, and 306 chlamydospores, respectively, although statistical evidence was not found.

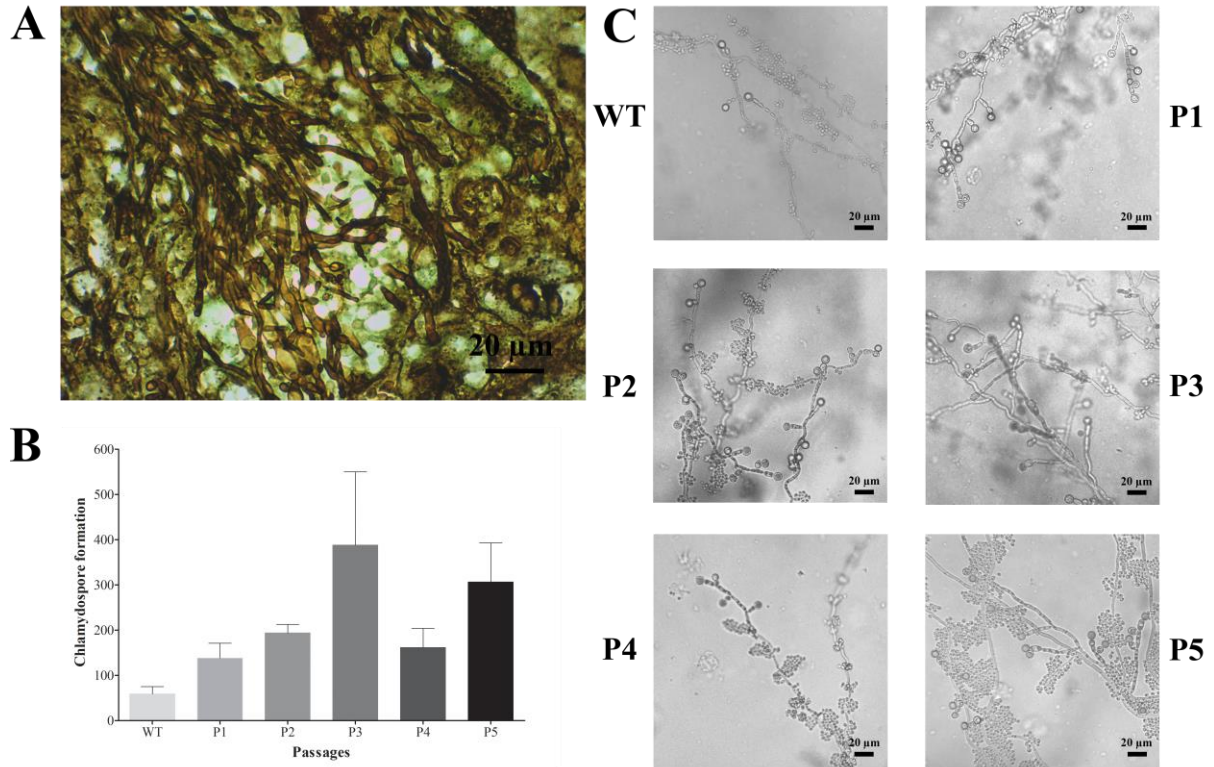


Figure 4. Influence of serial systemic candidiasis in chlamydospore production. (A) Kidney section stained with Gomori methenamine silver (GMS) showing a chlamydospore-like structure from kidney of infected murine. (B) Chlamydospore quantification assay in corn meal agar from wild-type SC5314 strain (WT) and passages (P1-P5) showing an increased trend in its production over passages. (C) Images from chlamydospore assay taken by optic microscope coupled with camera Moticam 5.0 MP at $\times 200$ magnification.

Filamentation rates from yeasts recovered after repeated passages

In our previous study, we demonstrated by proteomics, presence of several proteins related to yeast-to-hyphae transition. Thus, we performed a quantitative assessment of filamentous growth after incubation with FBS (Figure 5A). It is possible to observe an increasing trend in filamentation over the passages. A significant increase of filamentation was already observed during the first passage, from 14.5% for WT to 45.5% for P1 ($p < 0.0001$). Furthermore, significant differences were observed among P1 and the other passages (P2-P5), reaching 87% in P4 and 85% in P5 ($p < 0.05$). As we observe in Figure 5B through direct microscope and calcofluor white, majority presence of blastoconidia form in WT, and higher filamentous form in P1 to P5. Thus, these results suggest that the increased capacity to filament

could have contributed to the systemic infection observed through fungal burden and histopathological findings.

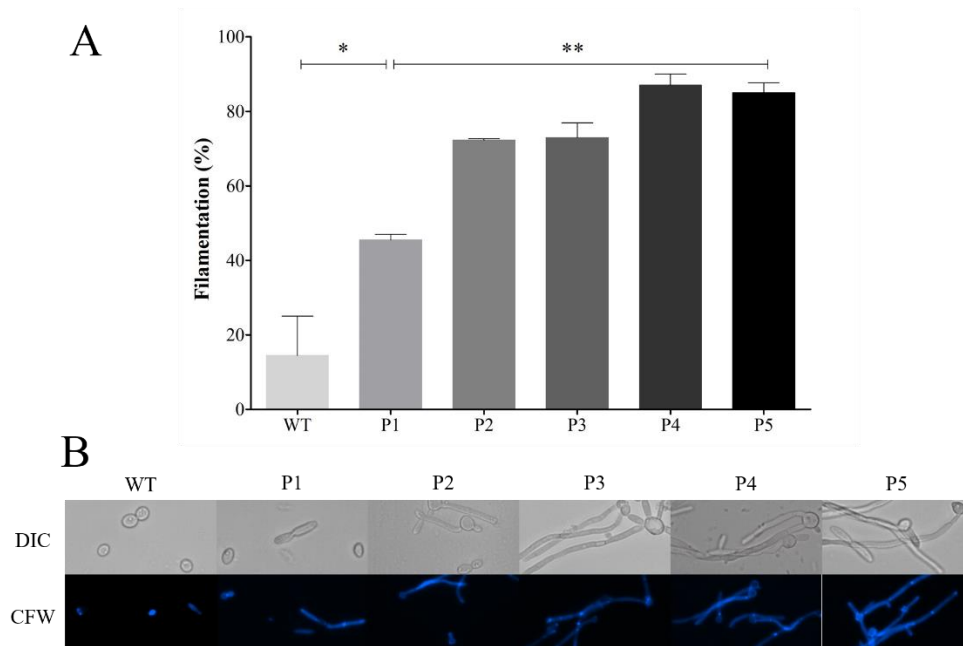


Figure 5. Filamentation profile increased in yeasts recovered from serial systemic infection caused by *C. albicans*. (A) Percentage of filamentation from wild-type SC5314 (WT) and passages 1 to 5 (P1-P5). An increased rate of hyphae formation is observed among the passages. (B) Differential interference contrast image (DIC) taken by optic microscope coupled with camera Moticam 5.0 MP under objective $\times 400$ and Calcofluor white (CFW) pictures from epifluorescence microscope represent blastoconidia and hyphae form observed during filamentation assay. * Statistical difference between WT and P1 ($p < 0.05$). ** Statistical differences between P1 and P2 to P5 ($p < 0.05$).

Secretion of phospholipase and proteinase *in vitro*

In addition to the filamentation, secretion of extracellular enzymes such as phospholipases and proteinases are important factors that contribute to the invasion of the tissue and development of infection [2, 4, 9, 12]. For phospholipase production, a significant reduction was detected in P1 and P2 ($p < 0.05$). After that, an increasing phospholipase activity was observed in P3 in relation to P2 that remained for the subsequent passages (Figure 6A). Regarding to proteinase assay (Figure 6B), P1 presented higher activity in relation to WT ($p < 0.05$) but from P2 to P5, the activities reduced significantly. These results demonstrate a modulation of extracellular enzymes activities during serial infection.

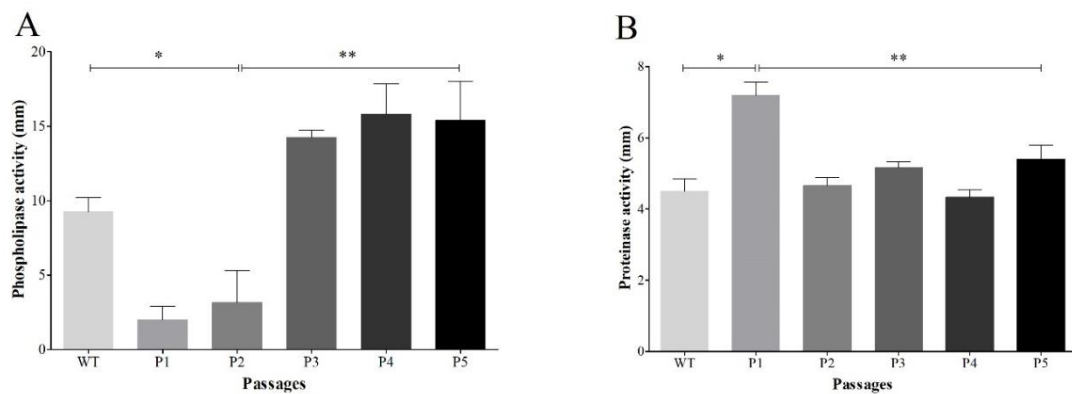


Figure 6. Extracellular enzymes of *Candida albicans* after successive exposure to the host. (A) Phospholipase activities for P1 and P2 decreased significantly, but the activity was recovered after P3, surpassing wild type. (B) Proteinase activity increased significantly in P1 but remained stable in the following passages. * $p < 0.05$ for isolates compared to WT. ** $p < 0.05$ for isolates compared among the passages.

Characterization of biofilm from yeasts isolated after serial infections

We found previously proteins with role in biofilm formation (unpublished observations). Therefore, to confirm the influence of serial passages in virulence profile during biofilm formation, we characterized biofilm by total biomass through crystal violet and CFU count (Figure 7 A & B). Furthermore, biofilm matrix was evaluated by carbohydrate and protein quantification (Figure 7 C & D). Our results demonstrated that it took one passage for yeast recovered from the tissue infected to increase both total biomass and CFU in relation to WT. From P2 onwards the results were maintained. Although there is no statistical evidence detected among passages, an increased trend was observed in both components.

Discussion

As *Candida* spp. have been one of the most common cause of nosocomial blood infections, being *C. albicans* the main pathogen associated to it, the continuous studies about pathogenicity of this microorganism are necessary [1, 15]. Our previous work has shown that the serial infection in a murine model of systemic candidiasis caused an increase in the virulence of yeasts recovered from this process demonstrated by the reduction in the median survival time over the passages (unpublished observations). Furthermore, proteomic analysis revealed several proteins related to virulence factors. Therefore, in this work, we aimed to confirm those findings by phenotype assays. First, we determined the fungal burden from different organs to verify the migration of yeast cells as a potential of infection and we found previously an overexpressed protein named yeast-form wall protein 1 (Ywp1) which is involved in decreasing adhesiveness,

but it can be related to enhancement ability to disseminate [32]. Thus, an increased fungal burden in different organs was observed, being kidneys the main affected organ (Figure 1) which led us to analyze histopathological of this organ as well as its profile of cytokines produced after each passage.

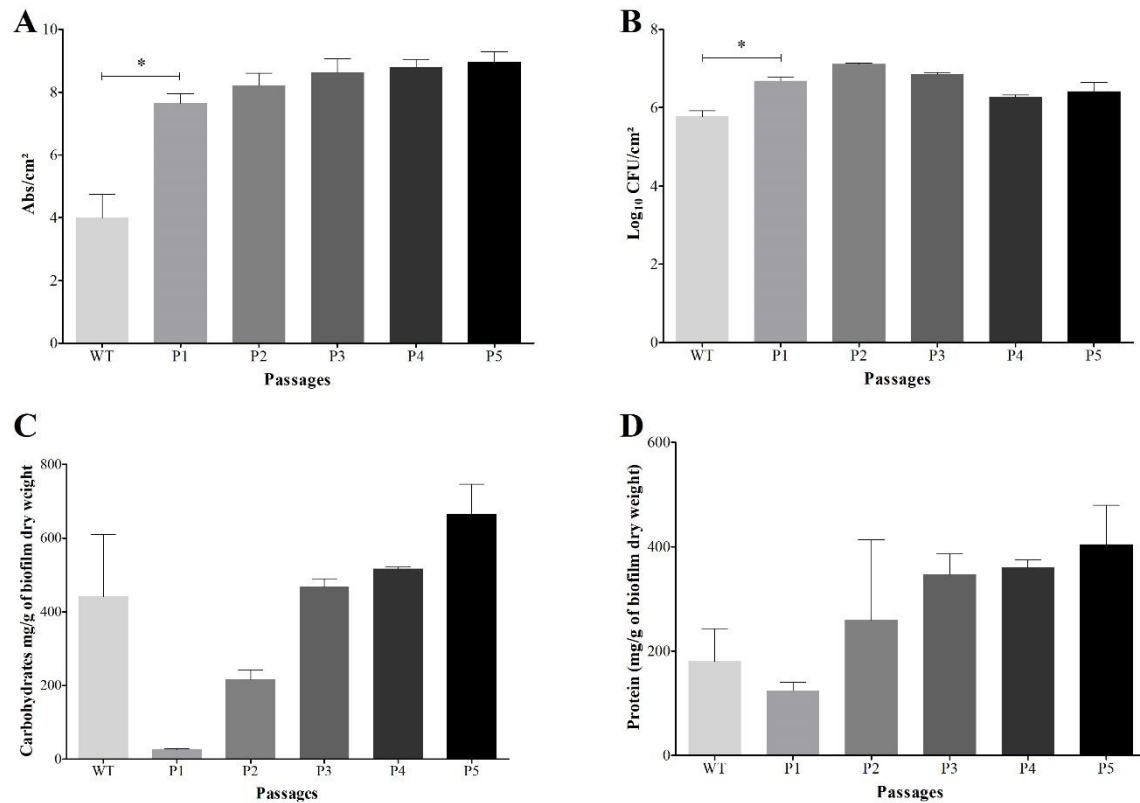


Figure 7. Biofilm formation increased since first passage in absorbance and CFU quantification. Biofilm characterization from wild-type SC5314 (WT) and isolates recovered from passages 1 to 5 (P1-P5). **(A)** Biofilm biomass total was quantified by absorbance in crystal violet and presented higher production since P1. **(B)** Logarithm of colony-forming unit (CFU) from biofilm was likewise significantly increased in P1. **(C)** Quantification of carbohydrates in biofilm matrix composition using phenol and sulfuric acid and glucose as a standard. **(D)** Quantification of protein in biofilm matrix composition using BCA reducing kit. * $p < 0.05$ for isolates compared to WT.

During dissemination of *C. albicans* in the host, we detected both blastoconidia and hyphae form in the kidneys (Figure 2) and evident presence of polymorphonuclear in all passages. Indeed, neutrophils are the major leukocytes found in the kidneys and are primordial for primary defense against fungal infections [33]. Additionally, the increased inflammatory response was confirmed by great release of proinflammatory cytokines TNF and IL-6 in serum and in the infected tissue, especially in P4, which coincides with the highest kidney burden among the passages. IL-6 is related to neutrophils recruitment and mice mutant IL-6 $-/-$ showed

lower circulating neutrophils and a reduced recruitment at the site of infection [34]. However, the immune response imbalance during infection, such as high levels of IL-6 can worsen the infection, leading to injuries, which could have happened during our study [35]. Similarly, the higher abundance in TNF levels in P4 may have contributed to the outcome of infection, although TNF has been shown to have a protective effect in decreasing fungal burden and enhancing phagocytosis by leukocytes [36, 37]. We believe that the challenge with *C. albicans* surpassed capacity of host response, maintaining a progressive infection throughout the experiment. Furthermore, these data gave us a support to investigate expression of virulence factors by *C. albicans* during serial passage in the host.

We detected the presence of a chlamydospore-like structure in the kidney in P3. Navarathna *et al.* [31] recovered chlamydospore from infected mouse kidneys and this data was a stimulus for the investigation of this structure in our study model. In the study cited, a mutant strain in chlamydospore formation (DLR6; $\Delta isw2/\Delta isw2$) was less virulent when compared to the group infected with WT strain, showing higher survival rate. They also suggest a possible role of chlamydospores in resisting to host defense. Therefore, our results of *in vitro* quantification of chlamydospore demonstrated an increasing trend in formation of such structures, highlighting P3 that coincides with the reduction in survival time of the infected animals (unpublished observations). Furthermore, these findings *in vitro* and above all the presence of chlamydospore in the tissue suggest a role of this structure in the virulence acquired over the passages (Figure 4).

The importance of yeast-to-hyphae transition is well established in the literature and experiments *in vitro* with mutant strains in hyphal formation demonstrated an attenuated virulence [4, 7, 8]. In our previous study, we identified many proteins associated to filamentation during the passages (unpublished observations). In this way, aiming to know how this change in morphology contributed with the increased virulence after serial infection, we determined the rate of filamentation from yeasts recovered after repeated passages incubated in a medium with FBS. We found higher rates of filamentation in recovered strains in comparison to WT (Figure 4) that may have influenced to the invasiveness of the tissue and development of the disease, leading to the increased virulence. Furthermore, these results emphasize the histopathological findings as hyphae forms were detected from P2 onwards (Figure 2). In addition, presence of proteins such as Nop1, Nop 58 and Sik1 with greater abundance in P1 (unpublished observations) were previously demonstrated to be overexpressed during early phase of filamentation [38]. This picture indicates transition to filamentous growth and correlate

with our findings *in vitro* as P1 has shown a significant increase of filamentation rates. Moreover, P4 also presented several proteins in higher abundance linked to this transition that can be associated with the raise in the rate of filamentation in relation to P1 and a reduction in the median survival time observed previously (unpublished observations).

Phospholipase and proteinases are hydrolytic enzymes secreted by *C. albicans* to contribute during tissue invasion [2, 4, 9-12]. Mandelblat *et al.* [13] found a higher phospholipase activity among strains of *C. albicans* recovered from patients with candidemia, denoting its important role in the pathogenicity. However, those strains did not present differences in the proteinase activity when compared to strain from vaginal infections. Similarly, we found high phospholipase production after the third passage but low activity of proteinase from P2 onwards. These results demonstrated a modulation of extracellular enzymes activities during serial infection. In addition, the higher activity found from P3 onwards could be related to the increased filamentation rates found during *in vitro* assay (Figure 5) and higher fungal burden (Figure 2).

It is well known the greater capacity to form biofilm *in vitro* and *in vivo* by *C. albicans* [17, 18]. Furthermore, CVC has been associated with persistent candidemia, once systemic strains were associated with patients using this device, indicating a possible source of infection and supporting the hypothesis of biofilm presence [13, 19, 20]. It denoted the importance of biofilm formation as a virulence factor. When we analyzed proteins recovered from serial systemic infection by *C. albicans*, we identified several proteins associated with biofilm production, especially in P1 and P4 (unpublished observations). Therefore, in this study, we aimed to characterize biofilm formation *in vitro* by total biomass, CFU, and matrix composition. We found that it took one passage (P1) to yeast increase and maintain its capacity to produce biofilm in relation to WT. Taken together, the increased ability acquired to form biofilm after repeated infections was confirmed by our proteomics data found previously.

From our knowledge there are few studies describing serial infection of *C. albicans* in a murine model with phenotypic assays. In contrast with Cheng *et al.* [23] and in agreement with Lüttich *et al.* [24], we recovered yeast from kidney, as it is the main organ affected. Different from what Lüttich *et al.* [24] who found that although phenotypic variability occurred among strains recovered from passages, but the overall virulence remained as wild-type strain, we detected an increased virulence over the passages as we could observe the higher filamentation, production of phospholipase, biofilm formation and an increasing trend in chlamydospore formation. One of the reason of these differences is the use of a higher inoculum

by us led to a more severe infection in the animals and from them that we recovered colonies to make the inoculum instead of using strain from healthy mice or with a chronic infection as Lüttich *et al.* [24]. By this way, we suggest that these higher expressions of virulence factors over the passages influenced the reduction of survival time observed previously (unpublished observations).

Conclusion & future perspective

Altogether, a progressive infection was observed after serial passages in a murine model, evidenced by increased fungal burden, presence of greater inflammatory areas in the histopathological findings and release of proinflammatory cytokines. Phenotypic assays demonstrated an increased *C. albicans* virulence after serial systemic infection, particularly for filamentation and biofilm formation, insighted by proteomics data in our previous study (unpublished observations). Thus, as association between phenotypic profile and proteins expressed during the infection was observed, we suggest that those proteins should be further analyzed as potential virulence markers and consequently be a target for new antifungal agents.

Summary points

- An increased fungal burden was observed after serial systemic infection by *C. albicans*, with kidney as the main organ affected.
- Histopathological analysis demonstrated presence of blastoconidia and hyphae in the kidney with evident inflammatory infiltrate along the passages.
- High release of proinflammatory cytokines TNF and IL-6 in systemic and local immune responses.
- An increased trend in chlamydospore production *in vitro* from yeasts recovered after serial passages was detected.
- A significant increase of filamentation was already observed during the first passage.
- Phospholipase secretion was higher from P3 onwards.
- Proteinase production, overall, was stable during the passages.
- It took one passage for yeast recovered from infection to increase both total biomass and CFU in relation to WT and from P2 onwards the results were maintained.
- A positive correlation between proteomics data obtained previously and phenotypic assays were found in this study.

Financial & competing interests disclosure

This work was supported by the Coordenação de Aperfeiçoamento de Pessoal de Nível Superior (CAPES), Conselho Nacional de Desenvolvimento Científico e Tecnológico (CNPq) and Fundação Araucária. The authors have no other relevant affiliations or financial involvement with any organization or entity with a financial interest in or financial conflict with the subject matter or materials discussed in the manuscript apart from those disclosed.

No writing assistance was utilized in the production of this manuscript.

Ethical conduct of research

Experiments with animals were approved by the Ethics Committee for Animal Use of the State University of Maringá, Paraná, Brazil under the protocol number CEUA 7261020418 and are in accordance with the Brazil's National Council for the Control of Animal Experimentation (CONCEA). Animals were monitored daily throughout the experiment.

References

Papers of special note have been highlighted as: • of interest; •• of considerable interest

1. Lamothe F, Lockhart SR, Berkow E, Calandra T. Changes in the epidemiological landscape of invasive candidiasis. *J. Antimicrob. Chemother.* 73(1), i4–i13 (2018).
2. Calderone RA, Fonzi WA. Virulence factors of *Candida albicans*. *Trends Microbiol.* 9(7), 327-335 (2001).
 - Provides a good overview about virulence factors in *C. albicans*.
3. Hall RA, Noverr MC. Fungal interactions with the human host: exploring the spectrum of symbiosis. *Curr. Opin. Microbiol.* 40, 58-64 (2017).
4. Mayer FL, Wilson D, Hube B. *Candida albicans* pathogenicity mechanisms. *Virulence* 4(2), 119-128 (2013).
5. Coleman DA, Oh SH, Zhao X *et al.* Monoclonal antibodies specific for *Candida albicans* Als3 that immunolabel fungal cells *in vitro* and *in vivo* and block adhesion to host surfaces. *J. Microbiol. Methods* 78(1), 71-78 (2009).
6. Cota E, Hoyer LL. The *Candida albicans* agglutinin-like sequence family of adhesins: functional insights gained from structural analysis. *Future Microbiol.* 10(10), 1635-1648 (2015).
7. Lo HJ, Köhler JR, DiDomenico B, Loebenberg D, Cacciapuoti A, Fink GR. Nonfilamentous *C. albicans* mutants are avirulent. *Cell* 90(5), 939-949 (1997).

8. Bi S, Lv QZ, Wang TT et al. SDH2 is involved in proper hypha formation and virulence in *Candida albicans*. *Future Microbiol.* 13(10), 1141-1156 (2018).
9. Naglik JR, Challacombe SJ, Hube B. *Candida albicans* secreted aspartyl proteinases in virulence and pathogenesis. *Microbiol. Mol. Biol. Rev.* 67(3), 400-428 (2003).
 - Important review about proteinase production by *C. albicans*.
10. Felk A, Kretschmar M, Albrecht A et al. *Candida albicans* hyphal formation and the expression of the Efg1-regulated proteinases Sap4 to Sap6 are required for the invasion of parenchymal organs. *Infect. Immun.* 70(7), 3689-3700 (2002).
11. Leidich SD, Ibrahim AS, Fu Y et al. Cloning and disruption of caPLB1, a phospholipase B gene involved in the pathogenicity of *Candida albicans*. *J. Biol. Chem.* 273(40), 26078–26086 (1998).
12. Ghannoum MA. Potential role of phospholipases in virulence and fungal pathogenesis. *Clin. Microbiol. Rev.* 13(1), 122-143 (2000).
 - Describes a review about phospholipase secretion by *C. albicans*.
13. Mandelblat M, Frenkel M, Abbey D, Ben AR, Berman J, Segal E. Phenotypic and genotypic characteristics of *Candida albicans* isolates from bloodstream and mucosal infections. *Mycoses* 60(8), 534-545 (2017).
14. Canela HMS, Cardoso B, Vitali LH, Coelho HC, Martinez R, Ferreira MEDS. Prevalence, virulence factors and antifungal susceptibility of *Candida* spp. isolated from bloodstream infections in a tertiary care hospital in Brazil. *Mycoses* 61(1), 11-21 (2018).
15. Pfaller MA, Diekema DJ. Epidemiology of invasive candidiasis: a persistent public health problem. *Clin. Microbiol. Rev.* 20(1), 133-163 (2007).
16. Nett JE, Lepak AJ, Marchillo K, Andes DR. Time course global gene expression analysis of an *in vivo* *Candida* biofilm. *J. Infect. Dis.* 200(2), 307-313 (2009).
17. Tobaldini-Valerio FK, Bonfim-Mendonça PS, Rosseto HC et al. Propolis: a potential natural product to fight *Candida* species infections. *Future Microbiol.* 11(8), 1035-1046 (2016).
18. Seleem D, Benso B, Noguti J, Pardi V, Murata RM. *In vitro* and *in vivo* antifungal activity of lichochalcone-A against *Candida albicans* biofilms. *PLoS ONE* 11(6), e0157188 (2016).
19. Chen CY, Huang SY, Tsay W et al. Clinical characteristics of candidaemia in adults with haematological malignancy, and antimicrobial susceptibilities of the isolates at a medical centre in Taiwan, 2001–2010. *Int. J. Antimicrob. Agents* 40(6), 533-538 (2012).
20. Kang SJ, Kim SE, Kim UJ et al. Clinical characteristics and risk factors for mortality in adult patients with persistent candidemia. *J. Infect.* 75(3), 246-253 (2017).
21. Taff HT, Mitchell KF, Edward JA, Andes DR. Mechanisms of *Candida* biofilm drug resistance. *Future Microbiol.* 8(10), 1325-1337 (2013).

22. Cavaleiro M, Teixeira MC. *Candida* biofilms: threats, challenges, and promising strategies. *Front. Med.* 5, 28 (2018).
23. Cheng S, Clancy CJ, Zhang Z *et al.* Uncoupling of oxidative phosphorylation enables *Candida albicans* to resist killing by phagocytes and persist in tissue. *Cell. Microbiol.* 9(2), 492–502 (2007).
 - It is the First work regarding serial infection by *C. albicans* in a murine model.
24. Lüttich A, Brunke S, Hube B, Jacobsen ID. Serial passaging of *Candida albicans* in systemic murine infection suggests that the wild type strain SC5314 is well adapted to the murine kidney. *PLoS ONE* 8(5), e64482 (2013).
 - Describes phenotypic variability among strains recovered from serial passaging in a murine model of candidiasis, but without an overall change in the virulence.
25. Price MF, Wilkinson ID, Gentry LO. Plate method for detection of phospholipase activity in *Candida albicans*. *Sabouraudia* 20(1), 7-14 (1982).
26. Marcos-Arias C, Eraso E, Madariaga L, Aguirre JM, Quindós G. Phospholipase and proteinase activities of *Candida* isolates from denture wearers. *Mycoses* 54(4), e10-e16 (2011).
27. Alves CT, Ferreira ICFR, Barros L, Silva S, Azeredo J, Henriques M. Antifungal activity of phenolic compounds identified in flowers from north eastern Portugal against *Candida* species. *Future Microbiol.* 9(2), 139–146 (2014).
28. Silva S, Henriques M, Martins A, Oliveira R, Williams D, Azeredo J. Biofilms of non-*Candida albicans* *Candida* species: quantification, structure and matrix composition. *Med. Mycol.* 47(7), 681-689 (2009).
29. DuBois M, Gilles KA, Hamilton JK, Rebers PA, Smith F. Colorimetric method for determination of sugars and related substances. *Anal. Chem.* 28(3), 350–356 (1956).
30. Jacobsen ID, Lüttich A, Kurzai O, Hube B, Brock M. *In vivo* imaging of disseminated murine *Candida albicans* infection reveals unexpected host sites of fungal persistence during antifungal therapy. *J. Antimicrob. Chemother.* 69(10), 2785-2796 (2014).
31. Navarathna DHMLP, Pathirana RU, Lionakis MS, Nickerson KW, Roberts DD. *Candida albicans* ISW2 regulates chlamydospore suspensor cell formation and virulence in vivo in a mouse model of disseminated candidiasis. *PLoS ONE* 11(10), e0164449 (2016).
 - Proves the presence of chlamydospore in the kidneys and associates with virulence.
32. Gow NA, Brown AJ, Odds FC. Fungal morphogenesis and host invasion. *Curr. Opin. Microbiol.* 5(4), 366-371 (2002).
33. Lionakis MS, Lim JK, Lee CCR, Murphy PM. Organ-specific innate immune responses in a mouse model of invasive candidiasis. *J. Innate Immun.* 3(2), 180-99 (2011).
34. van Enckevort FH, Netea MG, Hermus AR *et al.* Increased susceptibility to systemic candidiasis in interleukin-6 deficient mice. *Med. Mycol.* 37(6), 419-426 (1999).

35. Chin VK, Foong KJ, Maha A, Rusliza B, Norhafizah M, Chong PP. Early expression of local cytokines during systemic *Candida albicans* infection in a murine intravenous challenge model. *Biomed. Rep.* 2(6), 869-874 (2014).
36. Louie A, Baltch AL, Smith RP *et al.* Tumor necrosis factor alpha has a protective role in a murine model of systemic candidiasis. *Infect. Immun.* 62(7), 2761-2772 (1994).
37. Cannom RR, French SW, Johnston D, Edwards JE Jr, Filler SG. *Candida albicans* stimulates local expression of leukocyte adhesion molecules and cytokines *in vivo*. *J. Infect. Dis.* 186(3), 389-396 (2002).
38. Rashki A, Ghalehnoo ZR, Dominguez R. The early response of *Candida albicans* filament induction is coupled with wholesale expression of the translation machinery. *Comp. Clin. Path.* 21(6), 1533-1545 (2012).

CHAPTER III

4. CONCLUSIONS

1. Murine model of serial systemic candidiasis was a useful tool for evaluating pathogenicity of *C. albicans*;
2. *C. albicans* acquired virulence after serial infection evidenced by reduction in survival time along passages;
3. An increased fungal burden was observed after serial infection, highlighting kidney as the main organ affected;
4. Histopathological analysis demonstrated presence of blastoconidia and hyphae in the kidney with evident inflammatory infiltrate along the passages;
5. High release of proinflammatory cytokines TNF and IL-6 in systemic and local immune responses;
6. Presence of chlamydospore-like structure *in vivo* and increased trending in chlamydospore production *in vitro*;
7. *C. albicans* recovered from infected tissue presented higher filamentation *in vitro* after passages;
8. Modulation of phospholipase and proteinase production during infection;
9. One passage was necessary to *C. albicans* acquire higher ability to produce biofilm;
10. A positive correlation between proteomics data and phenotypic findings were found in this study;
11. *C. albicans* presented an increased virulence potential after successive host-to-host passages.

5. FUTURE PERSPECTIVES

1. To select proteins with differential abundance among passages and to construct primers for their quantification by real time PCR;
2. To perform real time PCR for genes related to adhesion, phospholipase and proteinase activity;
3. To study specific proteins found during our experiments and evaluate its role in virulence during pathogenesis of *C. albicans*;
4. To evaluate other virulence factors such as phenotypic switching.